Data Supplement

TERT expression defines clinical outcome in pulmonary carcinoids

Lisa Werr, MD[1, 2], Christoph Bartenhagen, PhD[1,2], Carolina Rosswog, MD[1,2,3], Maria Cartolano, PhD[2,4], Catherine Voegele, PhD[5], Alexandra Sexton-Oates, PhD[5], Alex Di Genova, PhD[5], Angela Ernst[8], Yvonne Kahlert[1], Nadine Hemstedt[1], Stefanie Höppner, MD[1], Audrey Mansuet Lupo, MD[9], Giuseppe Pelosi, MD[10], Gudrun Absenger, MD[11], Janine Altmüller, MD[12], Jean-Philippe Berthet[13], Frederic Bibeau[14], Cécile Blanc Fourner[15], MD, Anne Boland, PhD[16], Christelle Bonnetaud, MD[17], Luka Brcic[18], Marie Brevet[19], Odd Terje Brustugun, MD, PhD[20-22], Giovanni Centonze, PhD[23], Lara Chalabreysse[19], Charlotte Cohen[13], Jean-Francois Deleuze, PhD[16], Jules L Derks, MD, PhD[24], Concetta Martina Di Micco[25], Anne-Marie C Dingemans[26], Élie Fadel[27], Paolo Graziano, MD[25], Paul Hofman, MD, PhD[26], Veronique Hofman[27], Stéphanie Lacomme[28], Marius Lund-Iversen[29], Jasna Metovic, MD[30], Massimo Milione, MD, PhD[23], Laura Moonen, MSc[24], Lucia Anna Muscarella, BSc-Phd[25], Peter Nürnberg, PhD[31], Robert Olaso, PhD[16], Vincent Meyer, PhD[16], Mauro Papotti, MD[30], Corinne Perrin[19], Gaetane Planchard[14], Helmut Popper[18], Nathalie Rousseau[15], Luca Roz[23], Giovanna Sabella[23], Angelo Sparaneo[25], Ernst Jan M Speel, PhD[24], Françoise Thivolet-Béjui[19], Vincent Thomas de Montpréville, MD[27], Jean-Michel Vignaud[28], Marco Volante, MD, PhD[30], Gavin M Wright, PhD[32], Francesca Damiola[33], Séverine Tabone-Eglinger[34], PharmD, PhD, Nicolas Girard, MD, PhD[35], Julie George, PhD[4, 36], Graziella Bosco, PhD[4], Alexander Quaas, MD[37], Laura H. Tang, MD, PhD[38], Kenneth Robzyk, PhD[39], Kyuichi Kadota, MD[40], Mee Sook Roh, MD[41], Rachel E. Fanaroff, MD[38], Christina J. Falcon, MPH[39], Reinhard Büttner, MD[37], Sylvie Lantuejoul, PhD[42], Natasha Rekhtman, MD, PhD[38], Charles Rudin, MD, PhD[43], William D. Travis, MD[38], Nicolas Alcala, PhD[5], Lynnette Fernandez-Cuesta, PhD[5], Matthieu Foll, PhD[5], Martin Peifer, PhD[2, 4], Roman K. Thomas, MD[4, 37*,#], Matthias Fischer, MD[1,2 *,#]

[*]*These authors contributed equally.*

Author affiliations:

[1] Department of Experimental Pediatric Oncology, University Children's Hospital of Cologne, Kerpener Str. 62, 50924 Cologne, Germany

[2] Center for Molecular Medicine Cologne (CMMC), Medical Faculty, University of Cologne, Kerpener Str. 62, 50924 Cologne, Germany

[3] Else Kröner Forschungskolleg Clonal Evolution in Cancer, University Hospital Cologne, Kerpener Str. 62, 50924 Cologne, Germany

[4] Department of Translational Genomics, University of Cologne, Faculty of Medicine and University Hospital Cologne, Weyertal 115b, 50931 Cologne, Germany

[5] Rare Cancers Genomics Team (RCG), Genomic Epidemiology Branch (GEM), International Agency for Research on Cancer/World Health Organisation (IARC/WHO), Lyon, 69008, France

[6] Instituto de Ciencias de la Ingeniería, Universidad de O'Higgins, Rancagua, Chile

[7] Centro de Modelamiento Matemático UMI-CNRS 2807, Universidad de Chile, Santiago, Chile

[8] Institute of Medical Statistics and Computational Biology, Medical Faculty, University of Cologne, 50924 Cologne, Germany

[9] Department of Pathology, Assistance Publique-Hôpitaux de Paris, Cochin Hospital, Paris Cité University, Paris, France

[10] Department of Oncology and Hemato-Oncology, University of Milan, Milan, Italy

[11] Division of Oncology, Department of Internal Medicine, Medical University of Graz, Graz, Austria

[12] Berlin Institute of Health at Charité - Universitätsmedizin Berlin, Core Facility Genomics, Charitéplatz 1, 10117 Berlin, Germany

[13] Department of Thoracic Surgery, FHU OncoAge, Nice Pasteur Hospital, University Cote d'Azur, Nice, France

[14] Pathology Department, Caen University Hospital, Normandy University, Caen, France

[15] Caen Lower Normandy Tumour Bank, Centre François Baclesse, Caen, France
[16] Université Paris-Saclay, CEA, Centre National de Recherche en Génomique Humaine (CNRGH), 91057, Evry, France
[17] FHU OncoAge, Biobank BB-0033-0025, Laboratory of Clinical and Experimental Pathology, Nice Pasteur Hospital, University Cote d'Azur, Nice, France
[18] Diagnostic and Research Institute of Pathology, Medical University of Graz, Graz, Austria
[19] Hospices Civils de Lyon, GHE, Institut de Pathologie Est, Bron, France
[20] Section of Oncology, Drammen Hospital - Vestre Viken Hospital Trust, Drammen, Norway & Institute of Clinical Medicine, Faculty of Medicine, University of Oslo, Oslo, Norway
[21] Department of Pathology, Oslo University Hospital, Oslo, Norway
[22] Section of Cancer Genetics, Dept of Cancer Research, Oslo University Hospital, Oslo, Norway
[23] Fondazione IRCCS Istituto Nazionale dei Tumori, Milan, Italy
[24] GROW School for Oncology and Reproduction, Maastricht University Medical Centre, Maastricht, The Netherlands
[25] Fondazione IRCCS Casa Sollievo della Sofferenza, San Giovanni Rotondo, Italy
[26] Department of Pulmonary Medicine, Erasmus MC Cancer Institute, University Medical Center, Rotterdam, The Netherlands
[27] Hôpital Marie-Lannelongue, Groupe Hospitalier Paris Saint Joseph, Le Plessis Robinson, France
[28] Nancy Regional University Hospital, CHRU, CRB Biobank-0033-00035, Nancy, France
[29] Department of Pathology, Oslo University Hospital, Oslo, Norway
[30] Department of Oncology, University of Turin, Torino, Italy
[31] Cologne Centre for Genomics (CCG) and Centre for Molecular Medicine Cologne (CMMC), University of Cologne, Cologne, Germany
[32] University of Melbourne Department of Surgery, St Vincent's Hospital, Melbourne, Australia & Division of Cancer Surgery, Peter MacCallum Cancer Centre, Melbourne, Australia
[33] Department of Biopathology, Centre Léon Bérard & Pathology Research Platform, Cancer Research Center of Lyon, Lyon, France
[34] Biological Resource Center, Centre Léon Bérard, Lyon, France
[35] Paris Saclay University, Versailles, France
[36] Department of Otorhinolaryngology, Head and Neck Surgery, University Hospital Cologne, 50937 Cologne, Germany
[37] Institute of Pathology, Faculty of Medicine and University Hospital Cologne, University of Cologne, Kerpener Str. 62,50931 Cologne, Germany
[38] Department of Pathology, Memorial Sloan Kettering Cancer Center, New York
[39] Sloan Kettering Institue, Memorial Sloan Kettering Cancer Center, New York
[40] Department of Pathology, Faculty of Medicine, Shimane University 89-1 Enya-cho, Izumo, 693-8501 Shimane, Japan
[41] Department of Pathology, Dong-A University College of Medicine 1,3-ga, Dongdaeshin-dong, Seo-gu Busan, South Korea
[42] Grenoble Alpes University, Department of Biopathology, Centre de Lutte Contre le Cancer UNICANCER Léon Bérard, Lyon France
[43] Thoracic Oncology Service, Department of Medicine, Memorial Sloan Kettering Cancer Center, New York

Contents

S4B: Bar chart for the prevalence of *TERT* expression subgroups (*TERT* high/low) within stage-defined subgroups (stage ≤ IIA/≥ IIB) in the test cohort.

S4C: Bar chart for the prevalence of *TERT* expression subgroups (*TERT* high/low) within stages I to IV in the test cohort.

S4D: Bar chart for the prevalence of *TERT* expression subgroups (*TERT* high/low) within histologically-defined subgroups (atypical/typical) in the validation cohort.

S4E: Bar chart for the prevalence of *TERT* expression subgroups (*TERT* high/low) within stage-defined subgroups (stage ≤ IIA/ ≥ IIB) in the validation cohort.

S4F: Bar chart for the prevalence of *TERT* expression subgroups (*TERT* high/low) within stages I to IV in the validation cohort.

S5A: Mixture model with two components to determine a *TERT* expression threshold based on neuroblastoma samples.

S5B: Kaplan-Meier estimates of overall survival in test cohort patients (n=72) according to classification using the NB-cutoff (*TERT* expression threshold = 7.58).

S5C: Kaplan-Meier estimates of overall survival in validation cohort patients (n=97) according to classification using the NB-cutoff (*TERT* expression threshold = 7.58).

S6A: Overall survival of patients was assessed in subgroups defined by *TERT*-high (*TERT* expression score >8.84) and *TERT*-low (*TERT* expression score ≦8.84) expression in the test cohort

S6B: Overall survival of patients was assessed in subgroups defined by *TERT*-high (*TERT* expression score >8.84) and *TERT*-low (*TERT* expression score ≦8.84) expression in the validation cohort

S7A: Overall survival of patients was assessed in subgroups defined by *TERT*-high (*TERT* expression score >8.17) and *TERT*-low (*TERT* expression score ≦8.17) expression in patients with stage I and II

S7B: Overall survival of patients was assessed in subgroups defined by *TERT*-high (*TERT* expression score >8.17) and *TERT*-low (*TERT* expression score ≦8.17) expression in patients with stage III and IV

S7C: Overall survival of patients was assessed in subgroups defined by *TERT*-high (*TERT* expression score >8.17) and *TERT*-low (*TERT* expression score ≦8.17) expression in patients with stage I to IIIA

S7D: Overall survival of patients was assessed in subgroups defined by *TERT*-high (*TERT* expression score >8.17) and *TERT*-low (*TERT* expression score ≦8.17) expression in patients with stage IIIB to IV

S8: Mutation plot of pulmonary carcinoids.

S9A: Copy number plot of pulmonary carcinoid genomes of the test cohort.

S9B: Correlation between *TERT* expression and copy number in the combined test and validation cohort.

S10: Average expression of genes in proximity to the *TERT* locus in *TERT*-high and *TERT*-low pulmonary carcinoid subgroups of the test and validation cohort.

S11A-C: Analysis of APB indicating ALT in carcinoid samples with low *TERT* expression (**A**), high *TERT* expression (**B**) and ALT-positive neuroblastoma (**C**).

S11D: Distribution of telomere length ratios computed from sequencing data in pulmonary carcinoid and neuroblastoma subgroups.

S12A: Boxplot indicating *MKI67* expression in *TERT*-high and *TERT*-low carcinoids of the test an validation cohort.

S12B: Correlation between *TERT* and *MKI67* expression levels in pulmonary carcinoids of the test and validation cohort.

S13A: Kaplan-Meier estimates of overall survival of test cohort patients according to *TERT* copy number status.

S13B: Kaplan-Meier estimates of overall survival of validation cohort patients according to *TERT* copy number status.

3. Supplementary Tables

Table S1: Information on validation cohort part 1 (stage, age, survival, histology, *TERT* expression).

Table S2: Information on validation cohort part 2 (stage, age, survival, histology, *TERT* expression).

Table S3: Crosstable for the occurrence of risk factors *TERT* expression (*TERT* high/low) and histology (atypical/typical carcinoids) within the test cohort.

Table S4: Crosstable for the occurrence of risk factors *TERT* expression (*TERT* high/low) and stage (≤ stage IIA/≥ stage IIB) within the test cohort.

Table S5: Crosstable for the occurrence of risk factors *TERT* expression (*TERT* high/low) and histology (atypical/typical carcinoids) within the validation cohort.

Table S6: Crosstable for the occurrence of risk factors *TERT* expression (*TERT* high/low) and stage (≤ stage IIA/≥ stage IIB) within the validation cohort.

Table S7: Univariate analysis for overall survival of the risk factors stage and histology

Table S8: Multivariable analysis for overall survival, considering the risk factors *TERT* expression, stage (≤II versus ≥III), and histology (backward selection)

Table S9: Multivariable analysis for overall survival, considering the risk factors *TERT* expression, stage (≤IIIA versus ≥IIIB), and histology (backward selection).

Table S10: Multivariable analysis for overall survival, considering the risk factors *TERT* expression, stage (≤IIA versus ≥IIB), and histology (backward selection); threshold based on neuroblastoma dataset (NB-cutoff).

Table S11: Multivariable analysis for overall survival, considering the risk factors *TERT* expression, stage (≤II versus ≥III), and histology (backward selection)

Table S12: Multivariable analysis for overall survival, considering the risk factors *TERT* expression, stage (≤IIIA versus ≥IIIB), and histology (backward selection).

Table S13: Information on *TERT* copy number status (validation cohort).

Table S14: Crosstable for the occurrence of *TERT* expression (*TERT* high/low) and *TERT* copy number (normal/amplified) within the validation cohort.

Table S15: *TERT* (cg11625005) methylation beta values of the test and validation cohort.

Supplementary Methods

RNA sequencing

RNA sequencing data of the test cohort were obtained from previously published studies. [1,2] For the validation cohort part 1, frozen samples were reviewed by an expert pathologist and most representative areas with at least 70% tumor content were selected for downstream RNA extraction using QIAGEN kits. Only RNA samples with a minimum RIN of 7 were used for sequencing analyses. RNAseq was performed in the Cologne Center for Genomics. Libraries were prepared from total RNA using the Illumina® TruSeq® stranded mRNA sample preparation kit. After library validation and quantification using the Agilent tape station, a pool of libraries were sequenced to 50 M reads on an Illumina NovaSeq 6000 sequencer with a PE100 protocol. For validation cohort part 2, RNA extraction from frozen tumor tissue was performed using RNeady Mini Kit followed by Illumina HiSeq sequencing. [3] Raw data processing, read mapping, and gene expression quantification of sequencing data of both cohorts were performed using the Magic-AceView analysis pipeline, as described previously. [4,5] The Magic analysis tool is accessible at ftp://ftp.ncbi.nlm.nih.gov/repository/acedb/Software/Magic; AceView served as primary transcriptome reference (http://www.aceview.org). *TERT* expression levels are given as $\log_2$(sFPKM; Fragments Per Kilobase of transcript per Million mapped reads). Immune cell abundance was measured with CIBERSORTx[6] using the LM22 signature gene file. The carcinoid and neuroblastoma RNA-seq data was processed with Kallisto (version 0.44.0), and FPKM gene expression values were used as input for CIBERSORTx. The analysis was run in absolute mode, with B-mode batch correction enabled, quantile normalization disabled, and 500 permutations. [6]

Identification of a natural *TERT* expression threshold

A *TERT* expression threshold was determined to separate samples with high- and low-*TERT* expression within the test cohort of pulmonary carcinoids. The threshold was calculated from a fitted mixture model of two normal distributions. The model fit was performed by expectation

maximization. Tumors having a posterior probability of at least 95% for the second component were considered as '*TERT*-high', the remaining cases as '*TERT*-low'. The lowest expression value in the '*TERT*-high' group was chosen as threshold.

The distributions of *TERT* expression levels in pulmonary carcinoids (test cohort) and neuroblastoma were compared by a two-sample Anderson-Darling (AD) test, which revealed that the distributions were not significantly different (**Figure S2A**, *P*=0.091, A=0.743; based on a significance level of 0.05, the null hypothesis (H_0= *TERT* expression in neuroblastomas and carcinoids have the same distribution) was not rejected). A two-sample Anderson-Darling test was also used to compare the observed *TERT* expression levels in the carcinoid test cohort to levels (n=1000) drawn from the mixed model of two normal distributions (test statistics, A=0.743, *P*=0.523, **Figure S2B**. Modeling the distribution of *TERT* expression levels by fitting a mixture model of two right-tailed gamma distributions revealed similar results (test statistics, A=0.591, *P*=0.656, **Figure S2C**). Data modeling and evaluation was performed using the functions 'normalmixEM' and 'gammamixEM' in the R package 'mixtools' (version 1.2.0) and the R package 'kSamples' (version 1.2-9).

Whole-genome and whole-exome sequencing data analysis

Whole-genome sequencing (WGS) and whole-exome sequencing data were obtained from previous studies[1,2] and reanalyzed. Data analysis and detection of somatic mutations were performed as described previously. [4,7] Copy number analysis was performed using Sclust[8]. Copy number ≥3 was considered as "amplified". For the validation cohort, whole-genome sequencing was performed by the Centre National de Recherche en Génomique Humaine (CNRGH, Institut de Biologie François Jacob, CEA, Evry, France) on 59 fresh-frozen pulmonary carcinoids and their matched normal tissue. After quality control, 1 µg of genomic DNA was used for library preparation for whole-genome sequencing, using the Illumina® TruSeq® DNA PCR-Free Library Preparation Kit (Illumina Inc., CA, USA), according to the manufacturer's instructions. After quality control and normalization, qualified libraries were sequenced on a HiSeqX5 platform from Illumina (Illumina Inc., CA, USA) as paired-end 150

bp reads. Sequence quality parameters were assessed throughout the sequencing run, and standard bioinformatics analysis of sequencing data was based on the Illumina pipeline to generate FASTQ files for each sample. WGS reads were mapped to the reference genome GRCh38 (with ALT and decoy contigs) using an in-house workflow (https://github.com/IARCbioinfo/alignment-nf, release v1.0), as described previously. [4] In summary, this workflow relies on the Nextflow domain-specific language, version 20.10.0.5430 and consists of four steps: reads mapping (software bwa76, version 0.7.15), duplicate marking (software samblaster, version 0.1.24), reads sorting (software sambamba, version 0.6.6), and base quality score recalibration using GATK, version 4.0.12. Somatic Copy Number Variants (CNVs) were called using the PURPLE software version 2.52, as implemented in a Nextflow workflow (https://github.com/IARCbioinfo/purple-nf, version 1.0).

Calculation of Telomere Length Ratios

Telomere length ratios were computed from whole-genome and whole-exome sequencing data by counting raw sequencing reads containing the telomere repeat sequence (TTAGGG)[4] or its reverse complement. The ratio between the tumor and matched normal tissue was determined and normalized to the absolute amount of sequenced DNA using the total amount of reads from the tumor and the normal tissue. [4,7]

Clinical data

Clinical data for survival analyses of the test cohort was obtained from previously published datasets. [1,2] Information on Union for International Cancer Control (UICC)/American Joint Committee on Cancer stage, histology and survival (calculated in months from surgery to last day of follow-up or death) were used for the analyses. In order to improve the power of Kaplan-Meier analyses, patients were regrouped for UICC stage I-IV and UICC subgroups were not used. In addition, clinical stages were summarized into two prognostic groups: (i) ≦ UICC stage IIA, and (ii) ≧UICC stage IIB. [9-11] For the patients of the validation cohort, information on age,

sex, histological classification and stage were available (Table S1 and S2). Overall survival data was available for 72 patients of the test cohort and for 97 patients of the validation cohort.

Detection of alternative lengthening of telomeres (ALT)

Activation of ALT was determined by identification of ALT-associated promyelocytic leukemia (PML) nuclear bodies (APB), as assessed by 2–3 independent investigators using combined telomere fluorescence *in situ* hybridization and PML immunofluorescence as described previously. [7,12] An ALT-positive neuroblastoma sample was used as positive control.

Telomeric repeat amplification protocol assay

Telomerase activity was determined using the TeloTAGGG Telomerase PCR ELISAPLUS Kit (Sigma Aldrich, St. Louis, Missouri, USA), according to the manufacturer's protocol. Ten cryostat sections of 10 µm thickness (corresponding to approximately 10 mg tissue) from frozen tissue samples were used for the assay.

CD45 immunohistochemistry on fresh-frozen material (FF) tissue sections

Fresh frozen tumor sections (5 µM) were dried on superfrost slides for 30 minutes and fixed with cold acetone (-20°C) for 5 minutes. After drying, sections were rehydrated in 1x PBS for 10 minutes. Slides were incubated with CD45 antibody (Cellmarque, Cline 2B11/PD7/26; 1:100) diluted in blocking solution (1% BSA/1xTBS) for 45 minutes. After washing slides with 1x PBS (5 minutes), signals were detected using the EnVision™ G|2 System/AP, Rabbit/Mouse (Permanent Red; K5355). Slides were counterstained with hematoxylin and mounted with AquaTex (Sigma Aldrich, 1.08562). Slides were scanned using a BZ-X810 (Keyence) microscope at a 20x magnification.

DNA methylation profiling

DNA was isolated from snap-frozen tissue. Genome-wide DNA methylation was assessed using an Infinium HumanMethylation850 BeadChip (Illumina) according to the manufacturer's

instructions, as described previously. [2,4] Methylation data from the validation cohort was previously published and also assessed using the Illumina 450K platform. [3] Normalized methylation scores were computed using the R-package RnBeads (version 2.10.0).

Statistical analyses

SPSS (package release 27) and R (version 4.1.2) were used for statistical analyses. Survival was calculated as the time from diagnosis to death or last follow-up if the patient survived. Survival curves were estimated according to Kaplan-Meier and compared with the log-rank test. Estimates of 5-year survival rates are reported together with their standard errors. Associations of *TERT* expression status with clinical risk factors were examined using two-sided Fisher's exact test. Comparison of continuous variables, such as gene expression, was performed using two-tailed Mann-Whitney U test.

Multivariable analysis

After bivariate evaluation of associations between prognostic markers using Fisher's exact test, a test for multicollinearity was performed. Multivariable Cox regression models were used to analyze the simultaneous prognostic impact of *TERT* expression and established clinical markers (histology, typical versus atypical; stage, UICC stages ≦IIA versus ≧IIB[13], ≦III versus ≧III[14,15] and ≦IIIA versus ≧IIIB) on overall survival, including the possible interaction between *TERT* and histology. Statistically insignificant prognostic markers were excluded by applying backward elimination, according to likelihood ratio criteria (P entry <0.05, P removal ≧0.1).

Data availability

DNA methylation data has been deposited at the NCBI GEO database under Accession Number GSE261443. Sequencing and DNA methylation data from previously published studies reanalyzed in this study are available at EGA (EGAS00001003699, EGAS00001000650, EGAS00001000708 and EGAS00001000925) and the NCBI under GEO SuperSeries GSE118133. Newly generated sequencing data is available at EGA (EGAS00001005979).

Supplementary Figures

Figure S1. Comparison of the overall survival of the test and validation cohort

(A) Bar chart for the prevalence of atypical (AC) and typical (TC) carcinoids in the test and validation cohort

(B) Overall survival of patients of the test and validation cohort. Censored data are indicated by thick marks.

Figure S1

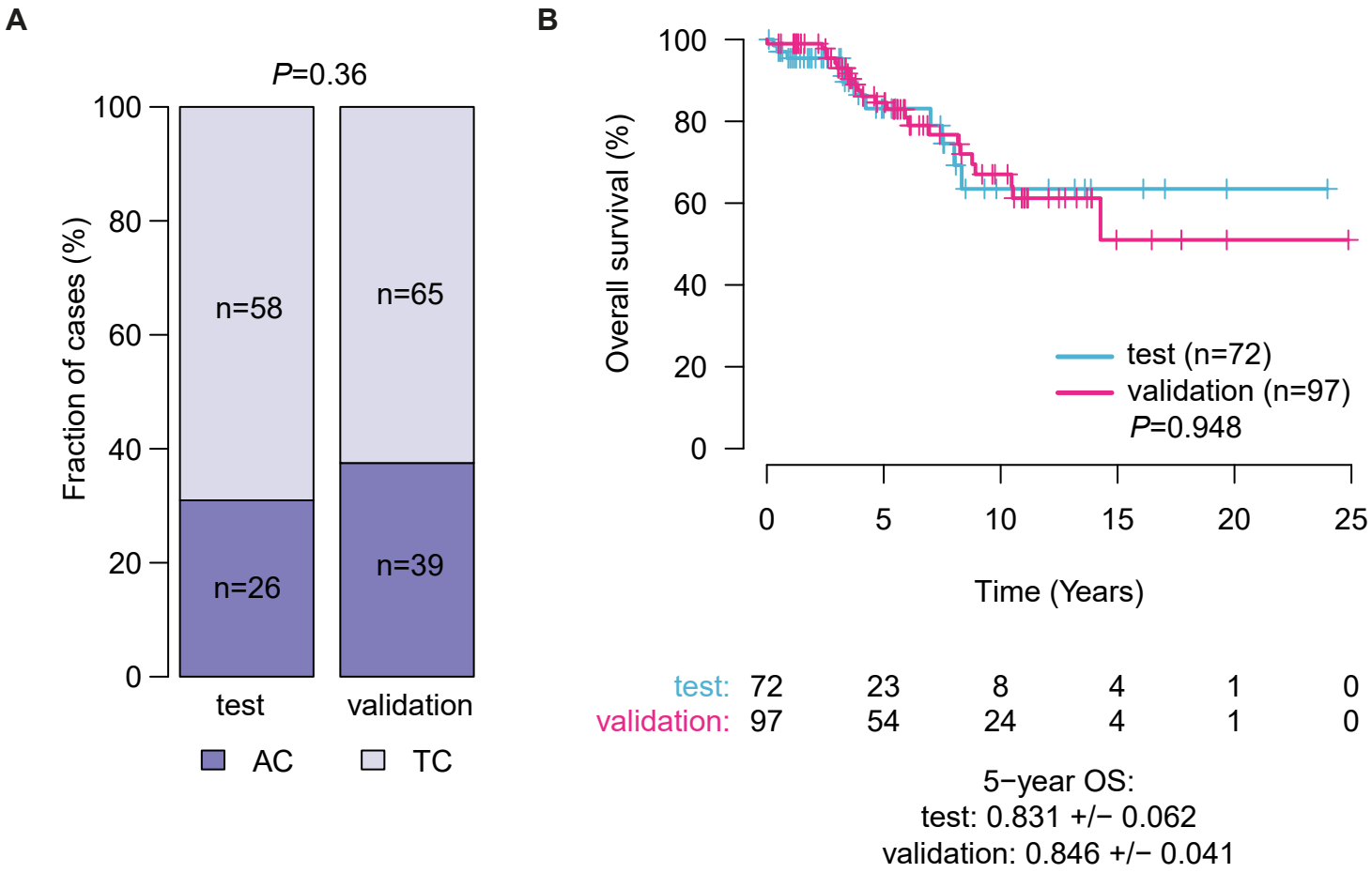
A
P=0.36
100
80
60
40
20
0
Fraction of cases (%)
n=58
n=26
n=65
n=39
test
validation
AC
TC
B
Overall survival (%)
test (n=72)
validation (n=97)
P=0.948
0
5
10
15
20
25
Time (Years)
test: 72 23 8 4 1 0
validation: 97 54 24 4 1 0
5−year OS:
test: 0.831 +/− 0.062
validation: 0.846 +/− 0.041

Figure S2. Comparison of *TERT* expression distributions in the test cohort of pulmonary carcinoids using two distinct mixture models.

Mixture models with two normal distributions (Panel A+B) or with two gamma components (Panel C) were applied to distinguish two subgroups with high and low *TERT* expression respectively in the test cohort of pulmonary carcinoids and in a neuroblastoma cohort. The distribution of *TERT* expression values is shown by the histogram (left axis), while curves indicate normal distributions fitted to tumors with low and high *TERT* expression using the mixture model (right axis). A two-sample Anderson-Darling test was used to compare both models. A comparison between the mixture model with two normal distributions of the test cohort of pulmonary carcinoids and the neuroblastoma cohort is shown in Panel A.

Figure S2

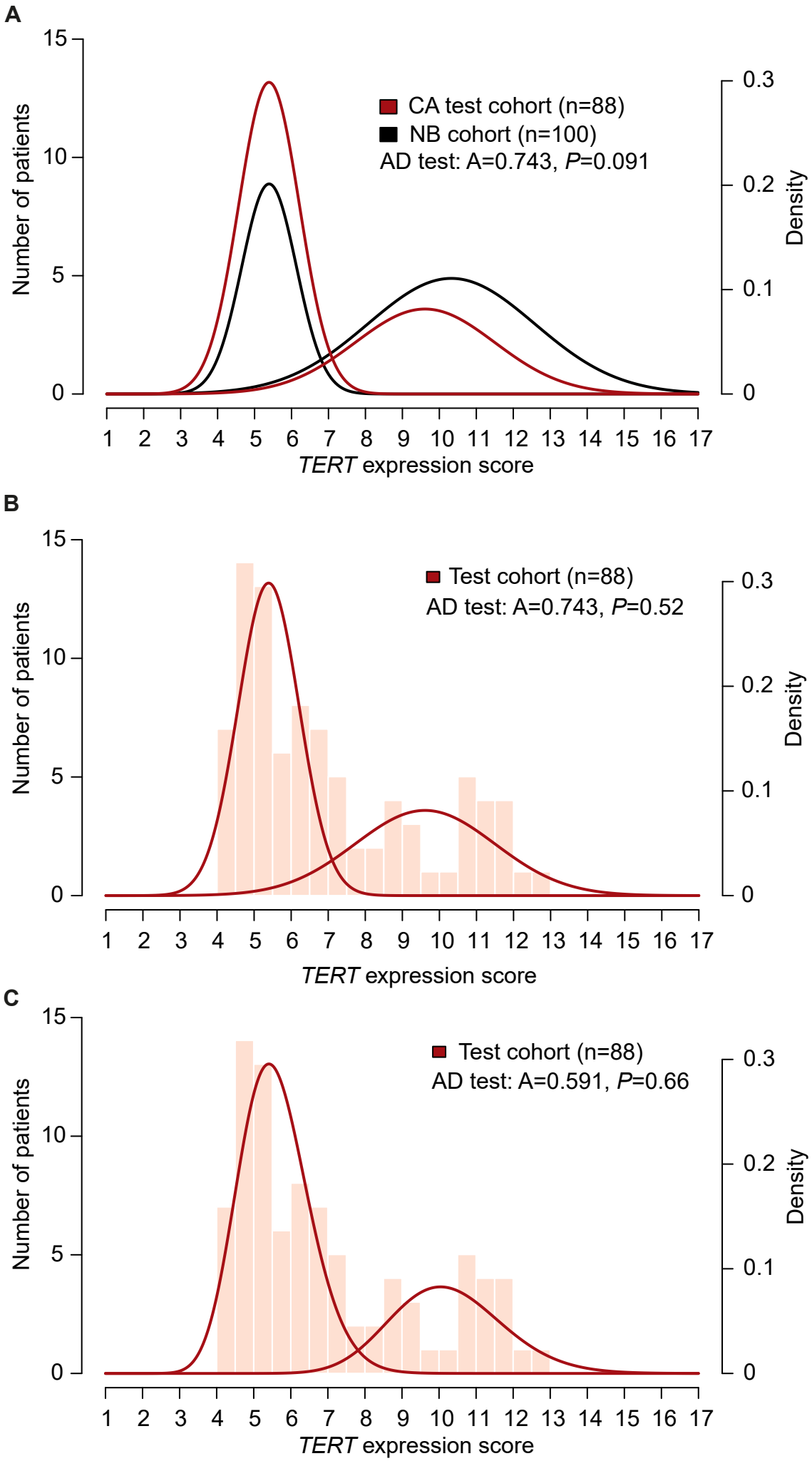
A
CA test cohort (n=88)
NB cohort (n=100)
AD test: A=0.743, P=0.091
Number of patients
Density
TERT expression score
B
Test cohort (n=88)
AD test: A=0.743, P=0.52
Number of patients
Density
TERT expression score
C
Test cohort (n=88)
AD test: A=0.591, P=0.66
Number of patients
Density
TERT expression score

Figure S3. Analysis of the immune cell infiltration in *TERT*-high and *TERT*-low pulmonary carcinods

(A) Boxplots showing the estimated total absolute proportion of immune cells in *TERT*-high and *TERT*-low carcinoids.
(B) Boxplots showing the estimated total absolute proportion of lymphocytes in *TERT*-high and *TERT*-low carcinoids.
(C) Absolute proportion of immune cells in *TERT*-high and *TERT*-low samples.
(D) HE and CD45 immunohistochemical staining of exemplary *TERT*-high and *TERT*-low carcinoids. Scale bars 100 µm.

Figure S3

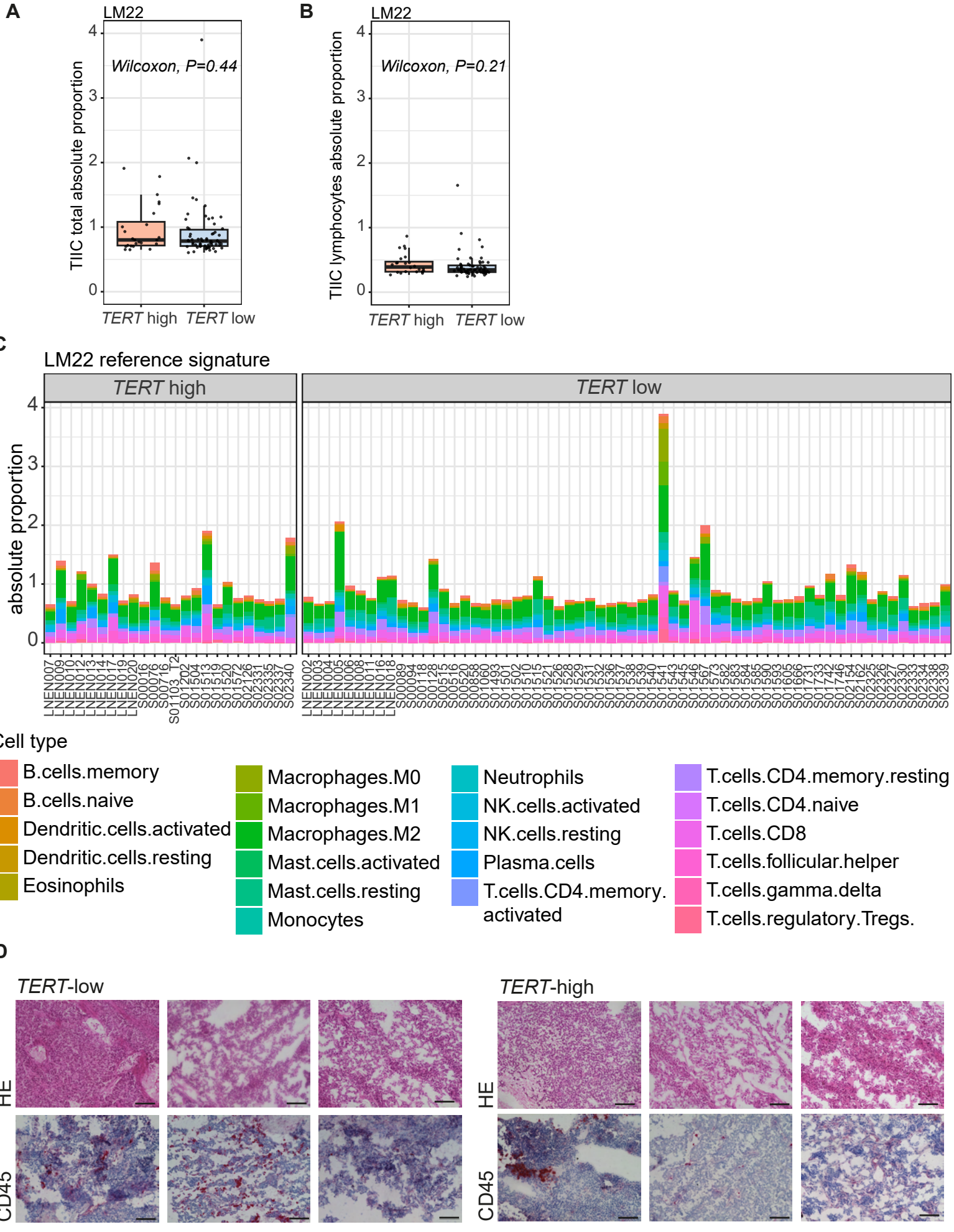
A
LM22
Wilcoxon, P=0.44
TIIC total absolute proportion
TERT high
TERT low
B
LM22
Wilcoxon, P=0.21
TIIC lymphocytes absolute proportion
TERT high
TERT low
C
LM22 reference signature
TERT high
TERT low
absolute proportion
Cell type
B.cells.memory
B.cells.naive
Dendritic.cells.activated
Dendritic.cells.resting
Eosinophils
Macrophages.M0
Macrophages.M1
Macrophages.M2
Mast.cells.activated
Mast.cells.resting
Monocytes
Neutrophils
NK.cells.activated
NK.cells.resting
Plasma.cells
T.cells.CD4.memory.activated
T.cells.CD4.memory.resting
T.cells.CD4.naive
T.cells.CD8
T.cells.follicular.helper
T.cells.gamma.delta
T.cells.regulatory.Tregs.
D
TERT-low
TERT-high
HE
CD45

Figure S4. Association of *TERT* expression-defined subgroups with established risk factors of pulmonary carcinoids.

Two-sided Fisher's exact test was used to determine the association of *TERT* expression-defined subgroups (*TERT*-high versus *TERT*-low) with the risk factors histology (typical versus atypical carcinoid) and stage (UICC stage ≤IIA versus ≥IIB) in the test (Panel A and B). The fraction of *TERT*-high and *TERT*-low carcinoids in stages !-IV are shown for the test (Panel C). Two-sided Fisher's exact test was used to determine the association of *TERT* expression-defined subgroups (*TERT*-high versus *TERT*-low) with the risk factors histology (typical versus atypical carcinoid) and stage (UICC stage ≤IIA versus ≥IIB) in the validation cohort (Panel D and E). The fraction of *TERT*-high and *TERT*-low carcinoids in stages !-IV are shown for the validation cohort (Panel F).

Figure S4

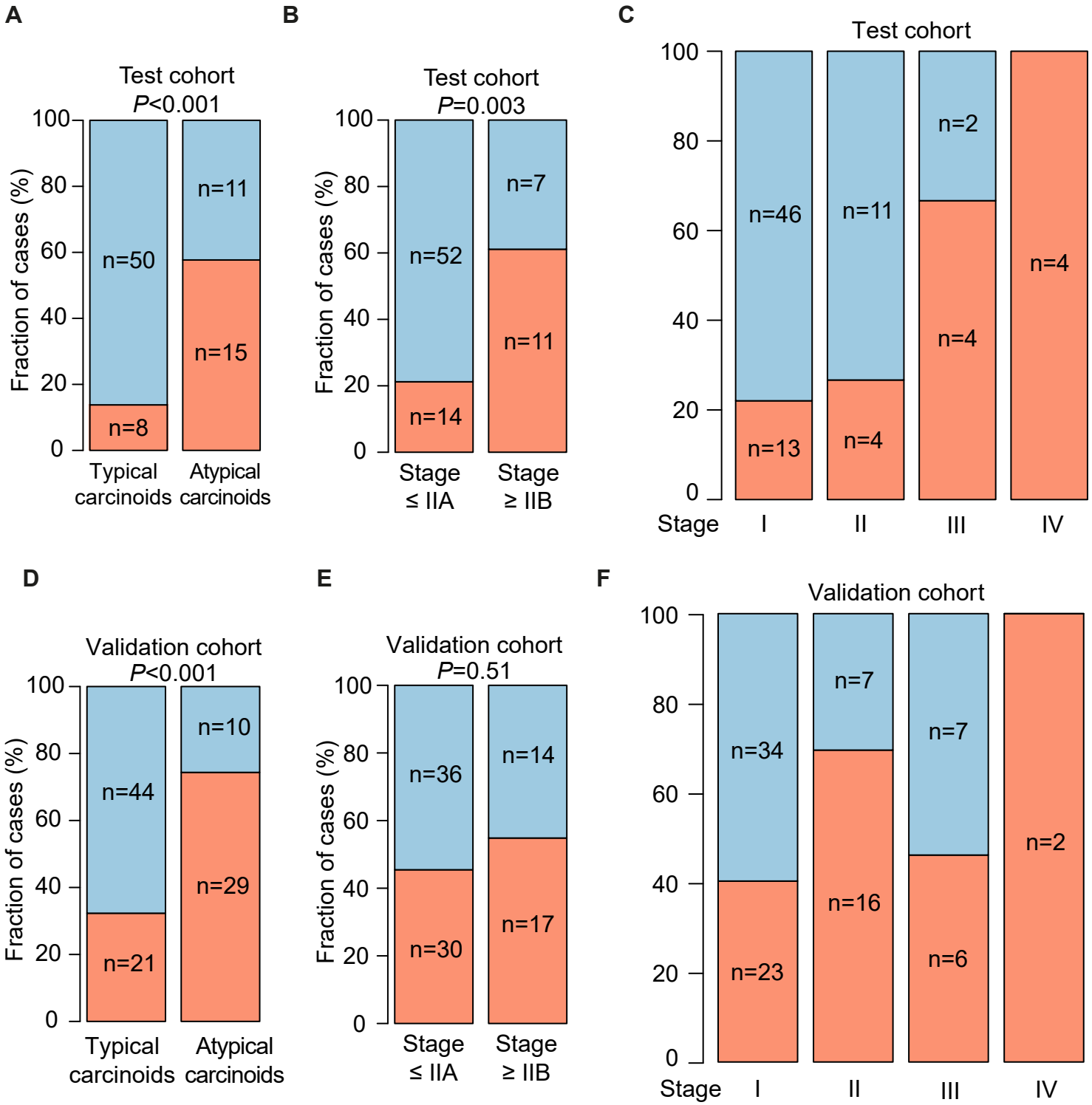
A
Test cohort
P<0.001
Fraction of cases (%)
100
80
60
40
20
0
n=50
n=8
n=11
n=15
Typical carcinoids
Atypical carcinoids
B
Test cohort
P=0.003
Fraction of cases (%)
n=52
n=14
n=7
n=11
Stage ≤ IIA
Stage ≥ IIB
C
Test cohort
n=46
n=13
n=11
n=4
n=2
n=4
Stage I II III IV
D
Validation cohort
P<0.001
Fraction of cases (%)
n=44
n=21
n=10
n=29
Typical carcinoids
Atypical carcinoids
E
Validation cohort
P=0.51
Fraction of cases (%)
n=36
n=30
n=14
n=17
Stage ≤ IIA
Stage ≥ IIB
F
Validation cohort
n=34
n=23
n=7
n=16
n=7
n=6
n=2
Stage I II III IV
TERT high
TERT low

Figure S5. Definition of a natural *TERT* expression cutoff from gene expression data of neuroblastoma samples.

The distribution of *TERT* expression values in the neuroblastoma cohort (n=100) is shown by the histogram (left axis), while curves indicate normal distributions fitted to tumors with low and high *TERT* expression using a mixture model (right axis). A threshold of a *TERT* expression score of 7.58 was determined to discriminate between samples with *TERT*-high versus *TERT*-low expression (Panel A). [16] Overall survival of patients with pulmonary carcinoids with high versus low *TERT* expression according to the previously defined *TERT* expression threshold of 7.58 in the test cohort (Panel B) and in the validation cohort (Panel C).

Figure S5

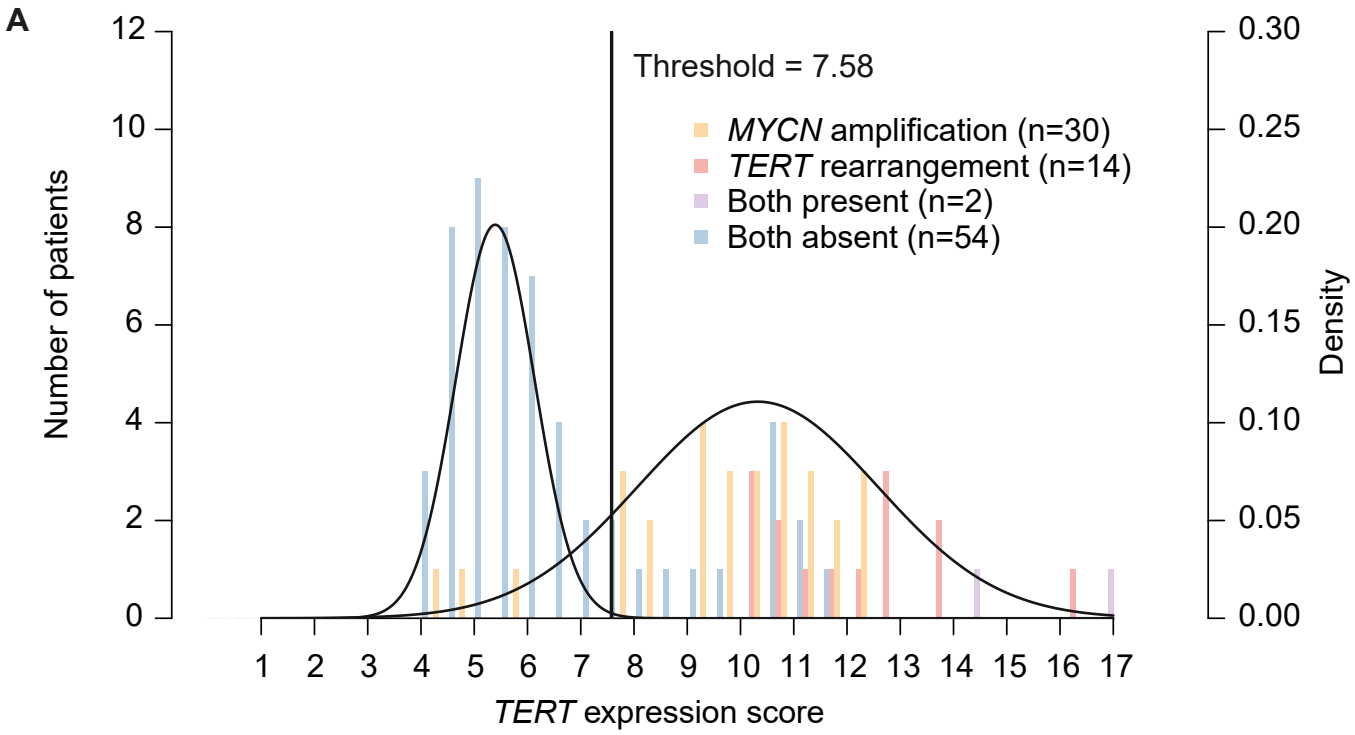
A
Threshold = 7.58
MYCN amplification (n=30)
TERT rearrangement (n=14)
Both present (n=2)
Both absent (n=54)
Number of patients
Density
TERT expression score

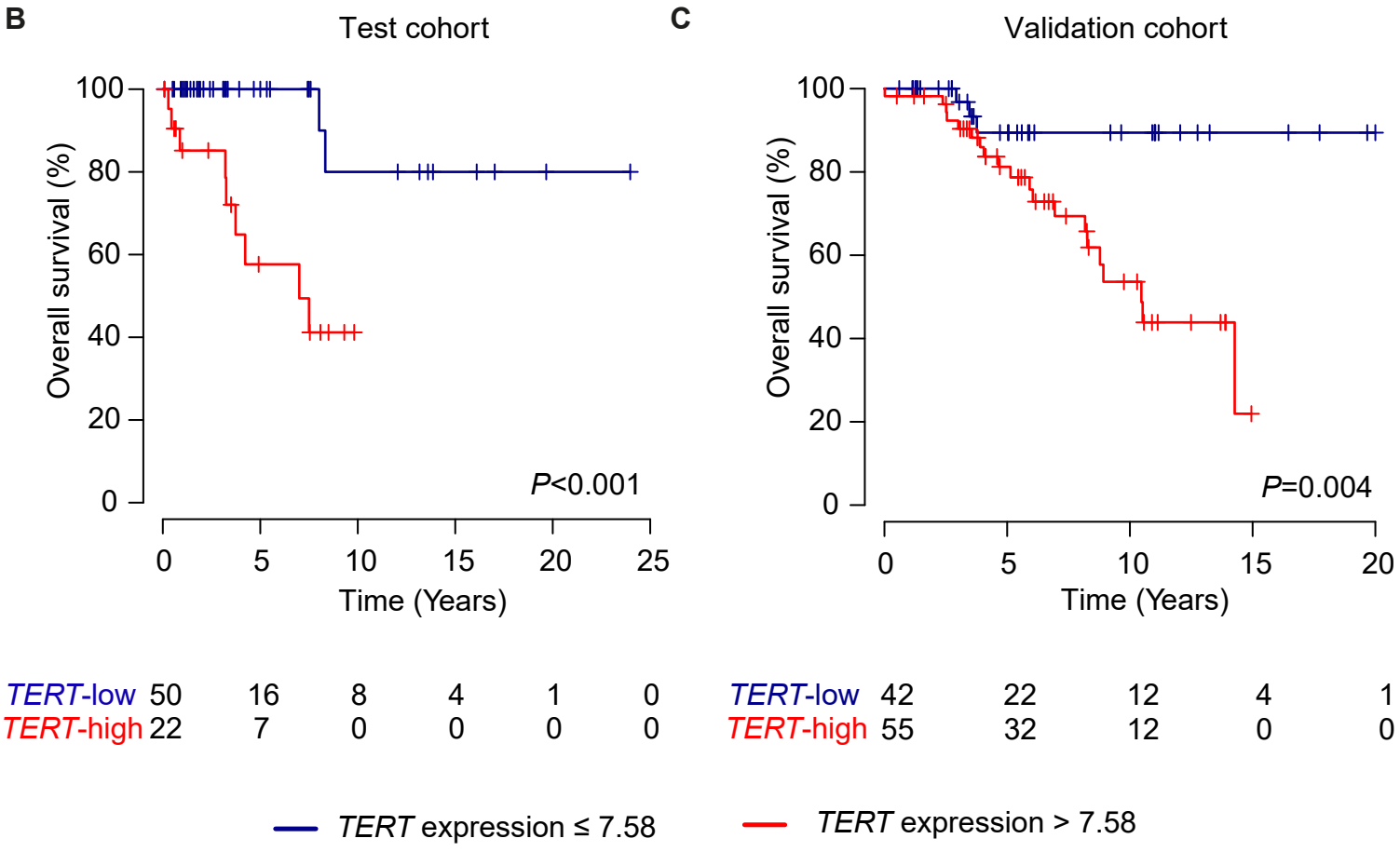
B
Test cohort
Overall survival (%)
P<0.001
Time (Years)
C
Validation cohort
Overall survival (%)
P=0.004
Time (Years)
TERT-low 50 16 8 4 1 0
TERT-high 22 7 0 0 0 0
TERT-low 42 22 12 4 1
TERT-high 55 32 12 0 0
TERT expression ≤ 7.58
TERT expression > 7.58

Figure S6: Kaplan-Meier plots of overall survival in patients with pulmonary carcinoids according to *TERT* expression (Kaplan-Meier scanning cut-off).

(A) Overall survival of patients was assessed in subgroups defined by *TERT*-high (*TERT* expression score >8.84) and *TERT*-low (*TERT* expression score ≦8.84) expression in the test cohort and (B) the validation cohort. Censored data are indicated by thick marks.

Figure S6

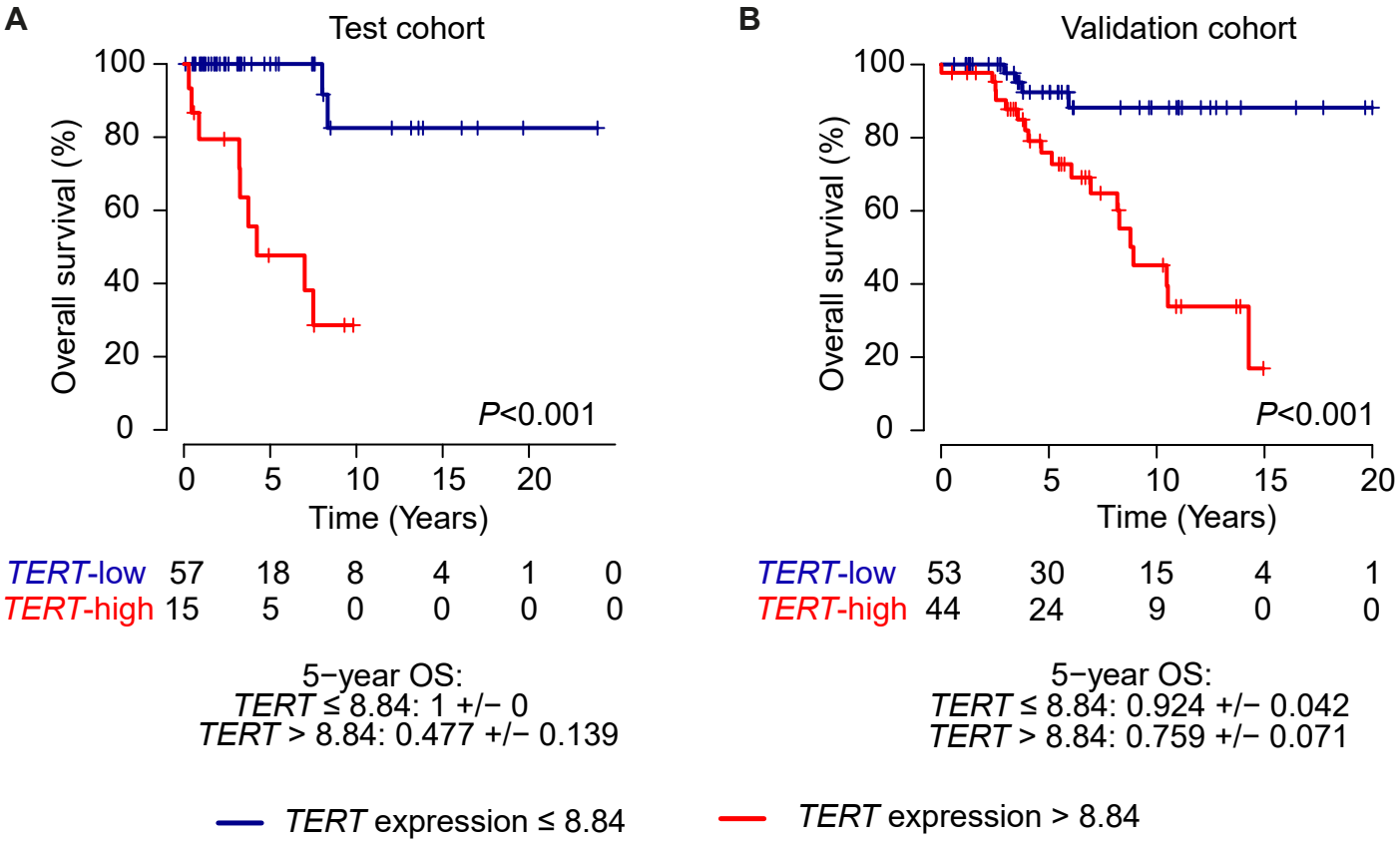
A
Test cohort
Overall survival (%)
100
80
60
40
20
0
P<0.001
0
5
10
15
20
Time (Years)
TERT-low 57 18 8 4 1 0
TERT-high 15 5 0 0 0 0
5−year OS:
TERT ≤ 8.84: 1 +/− 0
TERT > 8.84: 0.477 +/− 0.139
B
Validation cohort
Overall survival (%)
100
80
60
40
20
0
P<0.001
0
5
10
15
20
Time (Years)
TERT-low 53 30 15 4 1
TERT-high 44 24 9 0 0
5−year OS:
TERT ≤ 8.84: 0.924 +/− 0.042
TERT > 8.84: 0.759 +/− 0.071
TERT expression ≤ 8.84
TERT expression > 8.84

Figure S7. Kaplan-Meier plots of overall survival in patients with pulmonary carcinoids according to *TERT* expression in different stage categories.

(A) Overall survival of patients was assessed in subgroups defined by *TERT*-high (*TERT* expression score >8.17) and *TERT*-low (*TERT* expression score ≦8.17) expression in patients with stage I and II (A), stage III and IV (B), stage I to IIIA (C) and stage IIIB to IV (D). Censored data are indicated by thick marks.

Figure S7

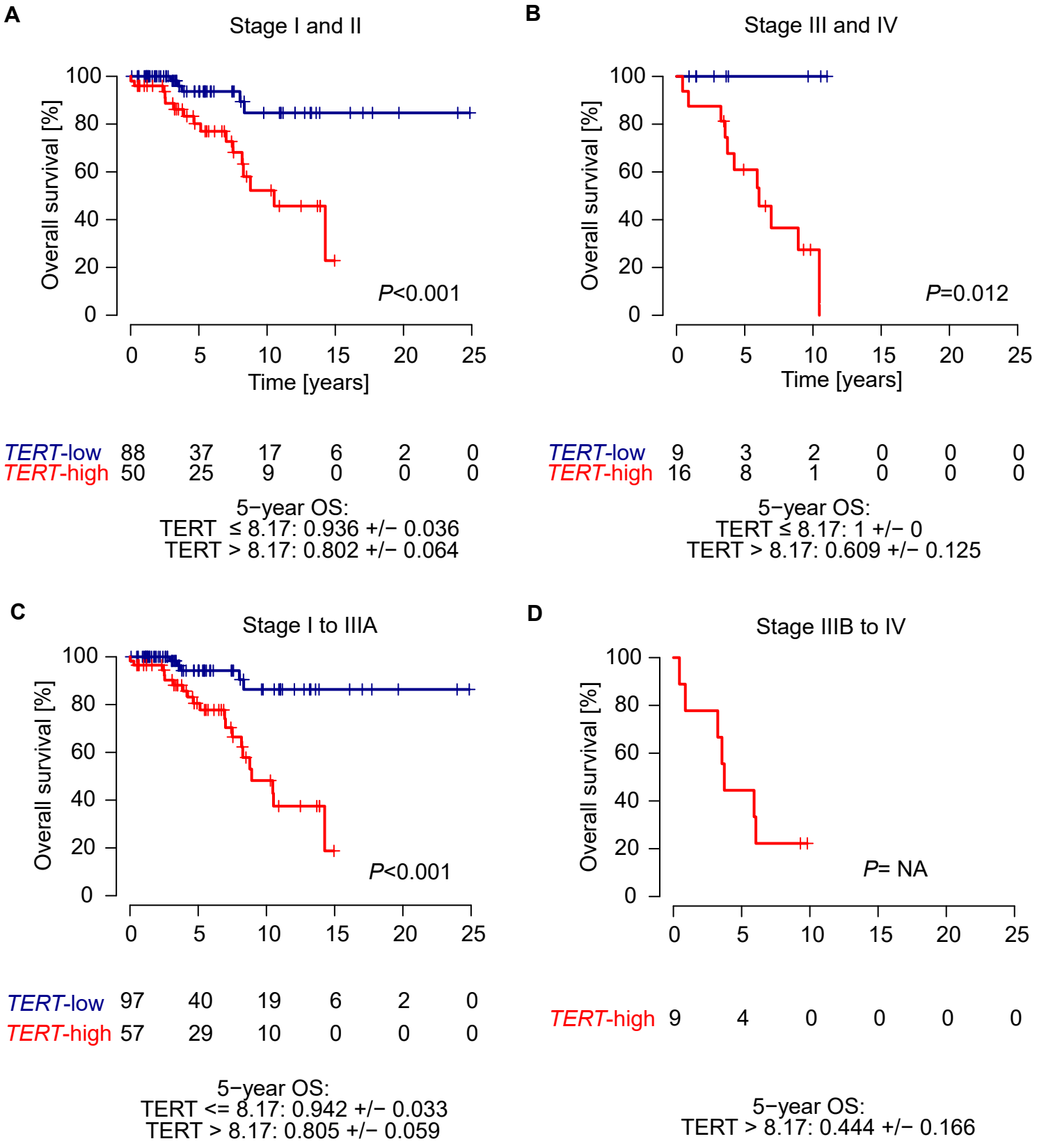
A
Stage I and II
Overall survival [%]
100
80
60
40
20
0
P<0.001
0
5
10
15
20
25
Time [years]
TERT-low 88 37 17 6 2 0
TERT-high 50 25 9 0 0 0
5−year OS:
TERT ≤ 8.17: 0.936 +/− 0.036
TERT > 8.17: 0.802 +/− 0.064
B
Stage III and IV
Overall survival [%]
P=0.012
Time [years]
TERT-low 9 3 2 0 0 0
TERT-high 16 8 1 0 0 0
5−year OS:
TERT ≤ 8.17: 1 +/− 0
TERT > 8.17: 0.609 +/− 0.125
C
Stage I to IIIA
Overall survival [%]
P<0.001
TERT-low 97 40 19 6 2 0
TERT-high 57 29 10 0 0 0
5−year OS:
TERT <= 8.17: 0.942 +/− 0.033
TERT > 8.17: 0.805 +/− 0.059
D
Stage IIIB to IV
Overall survival [%]
P= NA
TERT-high 9 4 0 0 0 0
5−year OS:
TERT > 8.17: 0.444 +/− 0.166

Figure S8. Somatic mutations detected in pulmonary carcinoids.

Non-synonymous somatic mutations detected in 47 pulmonary carcinoids of the test cohort for which WGS or WES data were available. Only mutations that occurred in at least two tumors samples are shown. Multiple mutations per gene in individual samples are indicated by horizontal black lines.

Figure S8

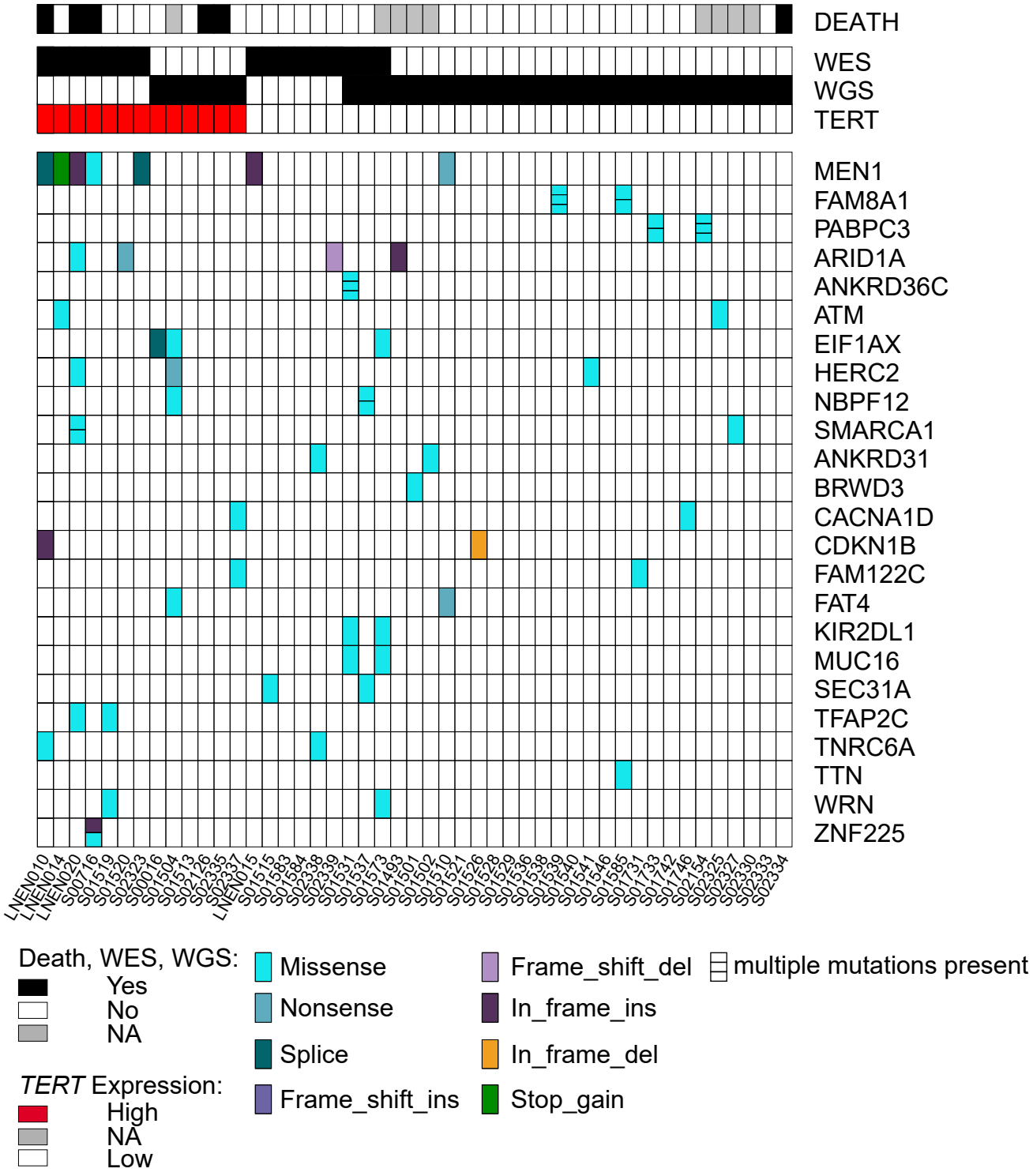
DEATH
WES
WGS
TERT
MEN1
FAM8A1
PABPC3
ARID1A
ANKRD36C
ATM
EIF1AX
HERC2
NBPF12
SMARCA1
ANKRD31
BRWD3
CACNA1D
CDKN1B
FAM122C
FAT4
KIR2DL1
MUC16
SEC31A
TFAP2C
TNRC6A
TTN
WRN
ZNF225
LNEN010
LNEN014
LNEN020
S00716
S01519
S01520
S02323
S00016
S01504
S01513
S02126
S02335
S02337
LNEN015
S01515
S01583
S01584
S02338
S02339
S01531
S01537
S01573
S01493
S01501
S01502
S01510
S01521
S01526
S01528
S01529
S01536
S01538
S01539
S01540
S01541
S01546
S01585
S01731
S01733
S01742
S01746
S02154
S02325
S02327
S02330
S02333
S02334
Death, WES, WGS:
Yes
No
NA
TERT Expression:
High
NA
Low
Missense
Nonsense
Splice
Frame_shift_ins
Frame_shift_del
In_frame_ins
In_frame_del
Stop_gain
multiple mutations present

Figure S9. Copy number variations in pulmonary carcinoids.

Copy number variations across the genome in pulmonary carcinoids of the test cohort (n=52) as determined by whole-genome or whole-exome sequencing (Panel A). Correlation of *TERT* expression and *TERT* copy numbers determined in samples of the test and validation cohort (Panel B).

Figure S9

A

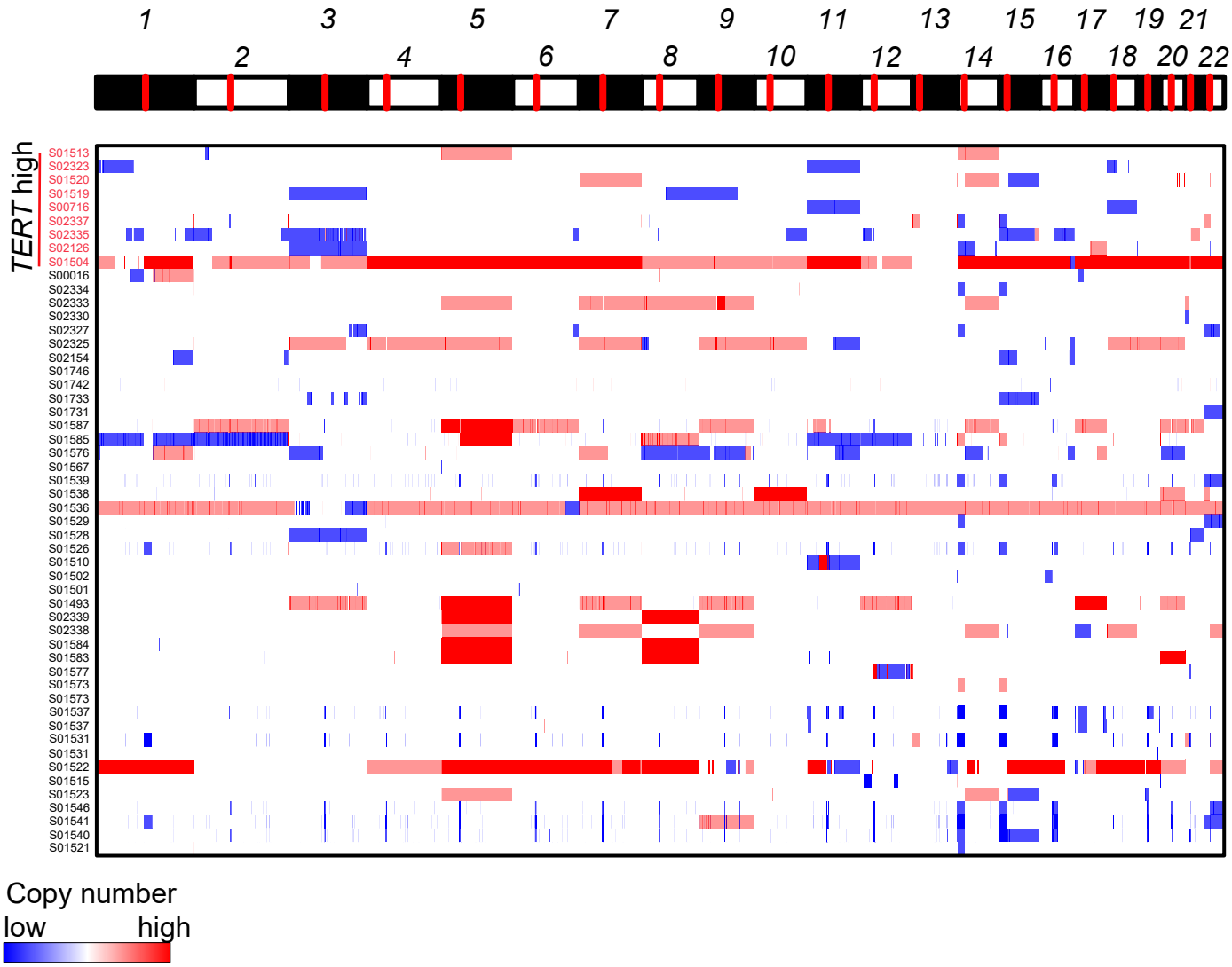
1 2 3 4 5 6 7 8 9 10 11 12 13 14 15 16 17 18 19 20 21 22
TERT high
S01513
S02323
S01520
S01519
S00716
S02337
S02335
S02126
S01504
S00016
S02334
S02333
S02330
S02327
S02325
S02154
S01746
S01742
S01733
S01731
S01587
S01585
S01576
S01567
S01539
S01538
S01536
S01529
S01528
S01526
S01510
S01502
S01501
S01493
S02339
S02338
S01584
S01583
S01577
S01573
S01573
S01537
S01537
S01531
S01531
S01522
S01515
S01523
S01546
S01541
S01540
S01521
Copy number
low
high

B

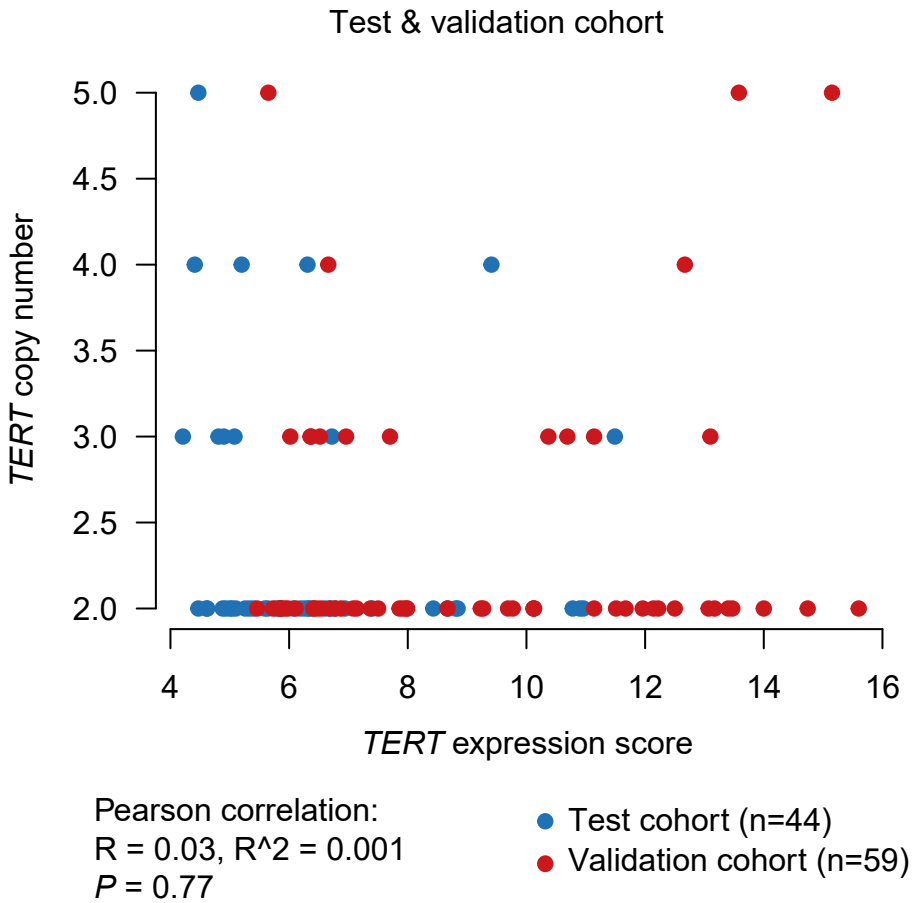
Test & validation cohort
TERT copy number
5.0
4.5
4.0
3.5
3.0
2.5
2.0
4
6
8
10
12
14
16
TERT expression score
Pearson correlation:
R = 0.03, R^2 = 0.001
P = 0.77
Test cohort (n=44)
Validation cohort (n=59)

Figure S10. Expression of genes encompassing the *TERT* locus in *TERT*-high and *TERT*-low pulmonary carcinoid subgroups.

Average expression of genes in proximity to the *TERT* locus in samples of the *TERT*-high versus *TERT*-low subgroup (Panel A).

Figure S10

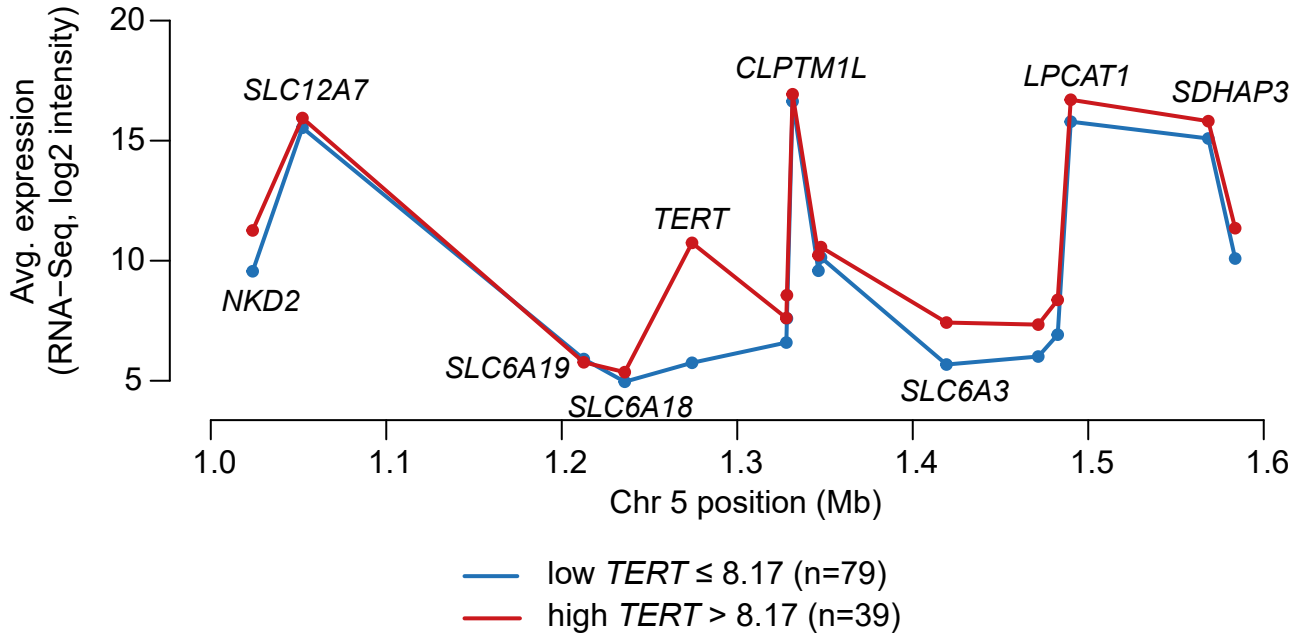
Avg. expression
(RNA−Seq, log2 intensity)
20
15
10
5
SLC12A7
NKD2
SLC6A19
SLC6A18
TERT
CLPTM1L
SLC6A3
LPCAT1
SDHAP3
1.0
1.1
1.2
1.3
1.4
1.5
1.6
Chr 5 position (Mb)
low TERT ≤ 8.17 (n=79)
high TERT > 8.17 (n=39)

Figure S11. Analysis of APB and telomere lengths in pulmonary carcinoids.

Telomere FISH (green) and PML immunofluorescence staining (red) for detection of APB as a marker of ALT is exemplarily shown in pulmonary carcinoids with low (Panel A) and high *TERT* expression (Panel B), and compared to an ALT-positive neuroblastoma sample (Panel C). Scale bars 10 µm. Distribution of telomere length ratios as computed from whole-genome and whole-exome sequencing data in *TERT*-high and *TERT*-low carcinoids compared to neuroblastoma lacking TMM (NB:TMM-), ALT-positive neuroblastoma (NB:ALT), and telomerase-positive neuroblastoma (NB:TERT; Panel D).

Figure S11

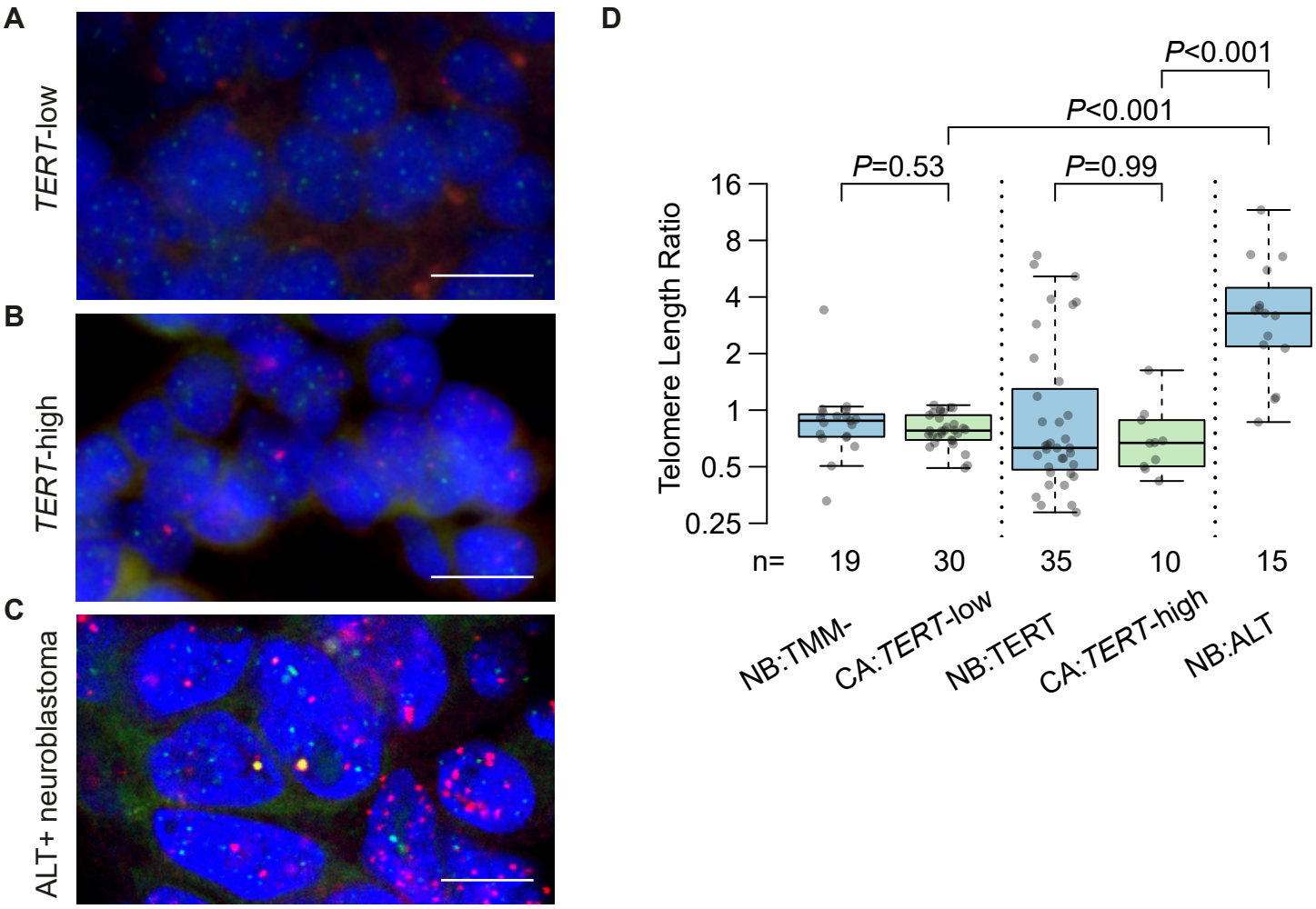
A
TERT-low
B
TERT-high
C
ALT+ neuroblastoma
D
P<0.001
P<0.001
P=0.53
P=0.99
Telomere Length Ratio
16
8
4
2
1
0.5
0.25
n=
19
30
35
10
15
NB:TMM-
CA:TERT-low
NB:TERT
CA:TERT-high
NB:ALT

Figure S12. *MKI67* expression in relation to *TERT* expression in pulmonary carcinoids.

MKI67 expression levels in *TERT*-high versus *TERT*-low carcinoids (Panel A), and correlation of *MKI67* and *TERT* expression levels (Panel B) in the test and validation cohort.

Figure S12

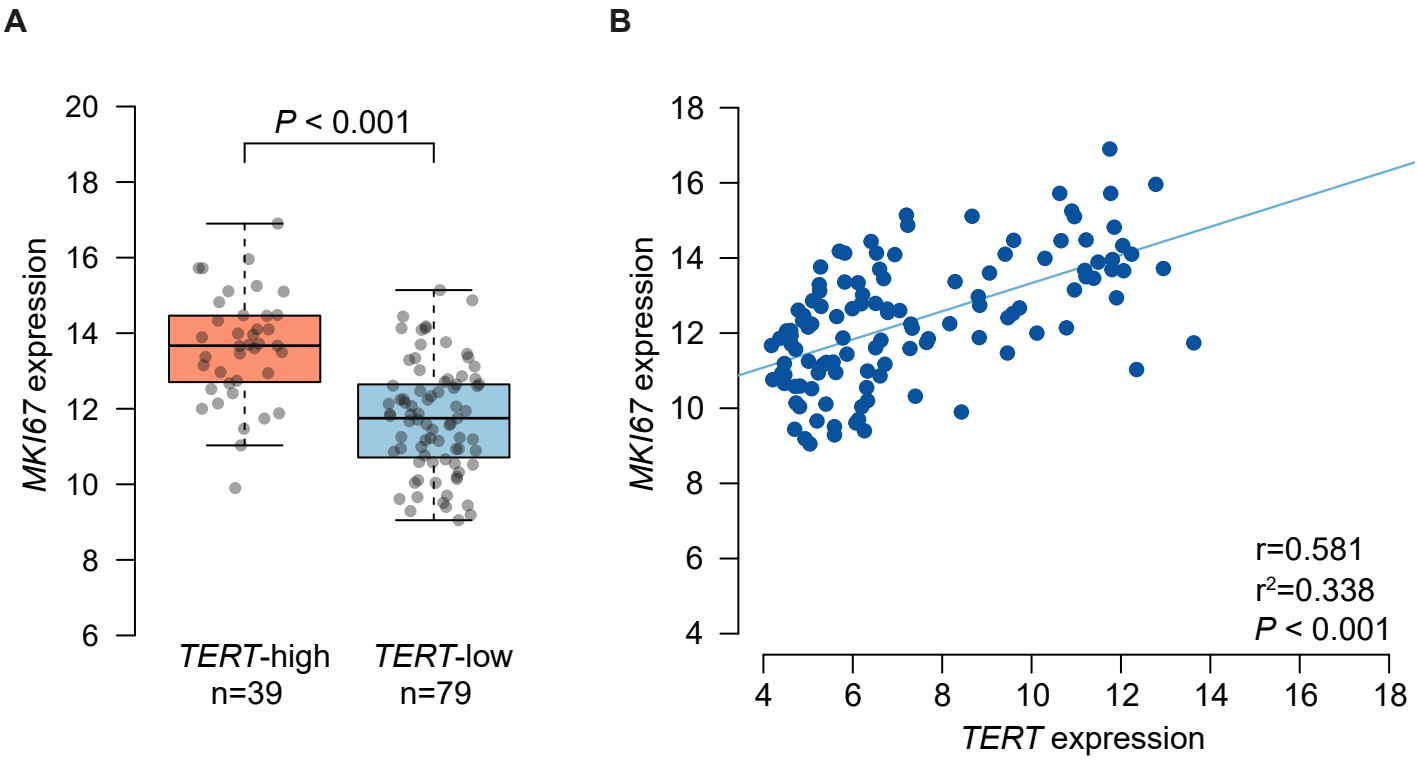
A
B
P < 0.001
MKI67 expression
TERT-high
n=39
TERT-low
n=79
TERT expression
r=0.581
r²=0.338
P < 0.001

Figure S13. Overall survival of pulmonary carcinoid patients according to *TERT* copy number status.

Kaplan-Meier estimates for overall survival of pulmonary carcinoid patients of the test (Panel A) and validation cohort (Panel B) according to the presence of absence of genomic *TERT* amplification.

Figure S13

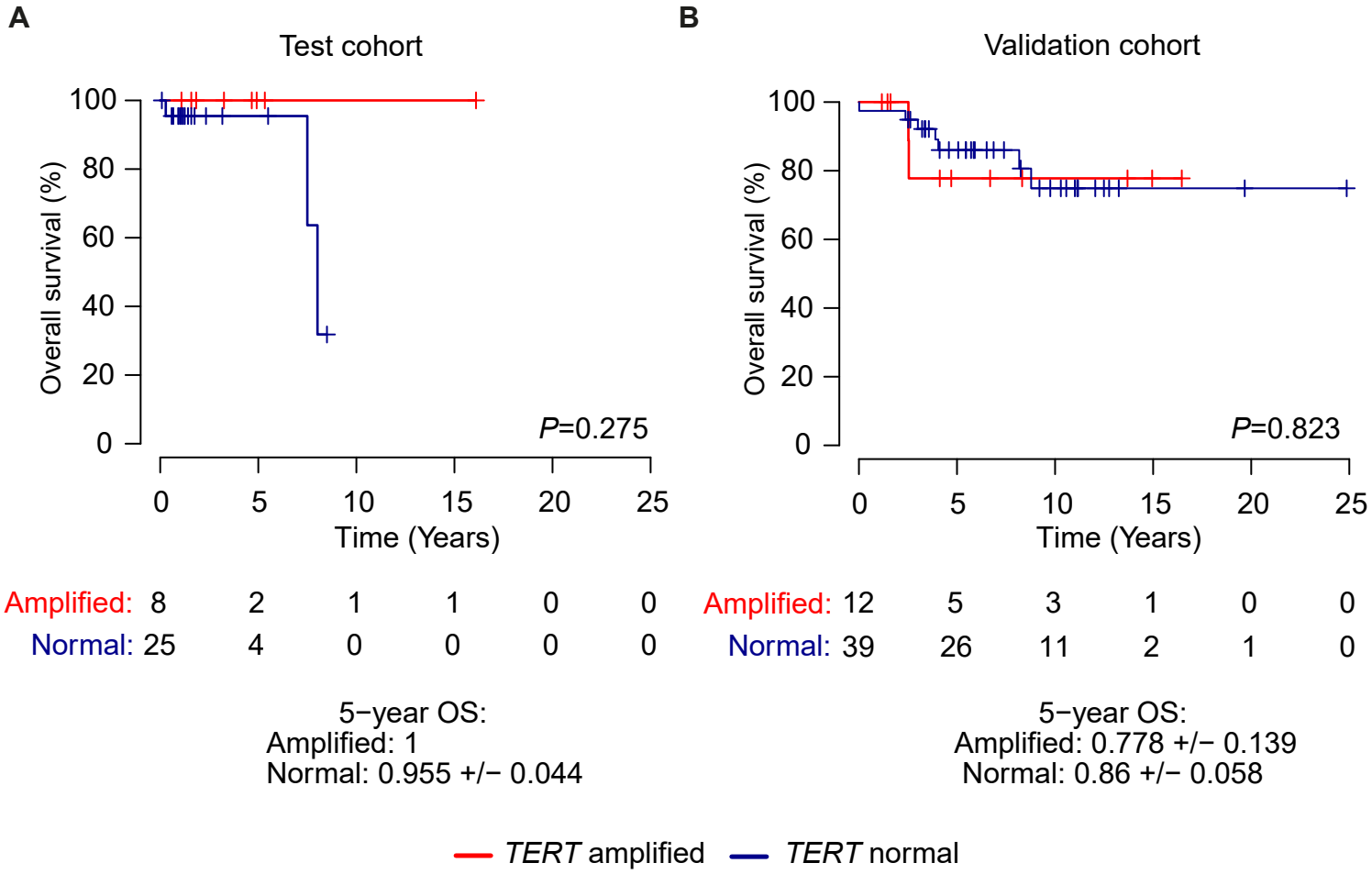
A
Test cohort
Overall survival (%)
100
80
60
40
20
0
P=0.275
0
5
10
15
20
25
Time (Years)
Amplified: 8 2 1 1 0 0
Normal: 25 4 0 0 0 0
5−year OS:
Amplified: 1
Normal: 0.955 +/− 0.044
B
Validation cohort
Overall survival (%)
100
80
60
40
20
0
P=0.823
0
5
10
15
20
25
Time (Years)
Amplified: 12 5 3 1 0 0
Normal: 39 26 11 2 1 0
5−year OS:
Amplified: 0.778 +/− 0.139
Normal: 0.86 +/− 0.058
TERT amplified
TERT normal

Supplementary Tables

Table S1: Information on validation cohort patients (sex, age, time of diagnosis/follow-up, survival) and tumors (histology, *TERT* expression).

Patient	Histo	Stage	Age	*TERT*	OS status	OS (bin)[#]	OS (days)	Surgery	Treatment type	Systemic Treatment*
LNEN044TU	Atypical	IIIB	75	8,34	dead	1	2160	lobectomy	radiotherapy + chemotherapy	1
LNEN047	Typical	IA2	66	5,65	alive	0	1719	lobectomy	none	0
LNEN048	NA	IA2	56	7,08	alive	0	1234	lobectomy	none	0
LNEN050TU	Atypical	IIIA	56	7,98	alive	0	3861	lobectomy	none	0
LNEN051TU	Atypical	IIB	62	7,7	alive	0	3039	segmentectomy	none	0
LNEN053TU	Typical	IIA	72	13,85	alive	0	184	lobectomy	none	0
LNEN054TU	Atypical	IA	44	8,8	alive	0	2248	lobectomy	none	0
LNEN055	Typical	IB	35	6,96	alive	0	427	lobectomy	none	0
LNEN056	Atypical	IIA	52	13,58	alive	0	1506	pneumonectomy	none	0
LNEN057	Atypical	IA3	37	12,67	alive	0	5460	segmentectomy	none	0
LNEN060	Typical	IIB	34	5,87	alive	0	2157	lobectomy	none	0
LNEN063	Atypical	IIB	62	12,5	dead	1	5	NA	none	0
LNEN064	Atypical	IIIA	51	13,17	alive	0	2379	NA	radiotherapy	0
LNEN066	Atypical		72	14	dead	1	1478	NA	radiotherapy	0
LNEN067	Atypical	IIB	80	14,74	dead	1	867	NA	none	0
LNEN068TU	Atypical	IA1	48	7,99	alive	0	1503	NA	none	0
LNEN069TU	Atypical	IIIA	46	6,58	alive	0	1328	NA	none	0
LNEN071	Atypical	IB	76	13,1	dead	1	929	NA	none	0
LNEN072	Atypical	IIB	67	10,69	alive	0	5001	NA	none	0
LNEN073TU	Atypical	IIIA	46	10,16	alive	0	1265	NA	none	0
LNEN074	Typical	IA1	50	5,83	alive	0	957	NA	none	0
LNEN076	Atypical	IB	72	11,51	alive	0	2088	lobectomy	none	0
LNEN077	Typical	IIB	45	12,14	alive	0	1225	pneumonectomy	none	0
LNEN081	Typical	IIB	38	7,14				segmentectomy	none	0
LNEN082TU	Atypical	IIB	65	12,02	alive	0	1384	lobectomy	none	0
LNEN083	Typical	IIB	67	12,22	alive	0	2508	lobectomy	somatostatin analog (ssa)	1
LNEN084	Atypical	IB	64	10,13	dead	1	1423	lobectomy	none	0
LNEN085TU	Typical	IIB	62	5,78	alive	0	220	lobectomy	none	0
LNEN086TU	Atypical	IIB	22	5,27	alive	0	2044	lobectomy	none	0
LNEN087TU	Atypical	IA1	69	6,3	dead	1	1068	lobectomy	none	0
LNEN089	Typical	IB/IIA	44	5,85				lobectomy	none	0
LNEN090TU	Typical	IV	66	9,27	dead	1	1300	lobectomy	none	0
LNEN091TU	Typical	IIIA	83	7,81	alive	0	1388	lobectomy	radiotherapy	0
LNEN092TU2	Atypical	IA	69	11,96	alive	0	3760	lobectomy	none	0
LNEN093TU1	Atypical	IIA	53	13,4	dead	1	2985	lobectomy	none	0
LNEN094TU5	Typical	IB	45	10,37	dead	1	921	lobectomy	none	0
LNEN095TU2	Typical	IB	79	15,15	alive	0	588	lobectomy	none	0

LNEN096TU3	Typical	IIIA	28	6,36	alive	0	533	lobectomy	none	0
LNEN097TU4	Typical	IA	72	6,41	alive	0	1849	lobectomy	none	0
LNEN100TU1	Typical	IA	68	7,92	alive	0	1989	lobectomy	none	0
LNEN103TU2	Typical	IA	51	8,56	alive	0	1717	wedge	none	0
LNEN104TU3	Typical	IA	56	6,87	alive	0	1849	lobectomy	none	0
LNEN106TU1	Atypical	IIA	67	13,47	alive	0	1675	lobectomy	none	0
LNEN107TU2	Typical	IIA	70	10,12	alive	0	916	lobectomy	none	0
LNEN108TU1	Typical	IA	81	9,77	alive			wedge	none	0
LNEN109TU	Typical	IA	74	5,93	alive	0	4839	lobectomy	none	0
LNEN110TU	Typical	IB/IIA	60	6,47	alive	0	9083	lobectomy	none	0
LNEN111TU2	Typical		65	6,78	alive	0	3362	lobectomy	NA	NA
LNEN112TU1	Typical		54	5,46	alive	0	7184	lobectomy	NA	NA
LNEN113TU2	Atypical		69	11,14	alive	0	4066	lobectomy	NA	NA
LNEN114TU3	Typical	IIB	54	5,98				lobectomy	NA	NA
LNEN115TU1	Typical		25	6,52	alive	0	6012	NA	NA	NA
LNEN116TU1	Atypical		74	15,6	dead	1	1098	pneumonectomy	NA	NA
LNEN117TU1	Typical	IA	62	5,73	alive	0	4659	lobectomy	NA	NA
LNEN118TU2	Atypical		40	6,37				NA	NA	NA
LNEN119TU3	Typical		59	6,66				NA	NA	NA
LNEN121TU	Typical	IA	42	7,37	alive	0	4401	lobectomy	none	0
LNEN122TU	Typical	IIIA	61	5,57	alive	0	3523	lobectomy	none	0
LNEN123TU	Typical	IB	56	7,86	alive	0	3563	lobectomy	none	0
LNEN125TU	Typical	IA1	44	11,67	alive	0	2701	segmentectomy	none	0
LNEN126TU	Typical	IIA	79	11,14	alive	0	2443	lobectomy	none	0
LNEN129TU	Typical	IA1	70	5,7	alive	0	805	lobectomy	none	0
LNEN130TU	Typical	IA3	66	6,41	alive	0	4080	lobectomy	none	0
LNEN132TU	Typical	IA	73	6,02	alive			lobectomy	none	0
LNEN133TU	Atypical	IB	70	13,07	dead	1	3207	pneumonectomy	none	0
LNEN135TU	Typical	IIB	74	7,5	alive	0	1302	lobectomy	none	0
LNEN136TU	Typical	IA1	55	9,23	alive	0	1176	lobectomy	none	0
LNEN137TU	Typical	IA1	44	9,71	alive	0	2036	lobectomy	none	0
LNEN139TU	Typical	IA1	63	9,27	alive	0	1995	lobectomy	none	0
LNEN140TU	Typical	IA1	62	6,54	alive	0	4021	segmentectomy	none	0
LNEN142TU	Typical	IA2	79	9,69	alive	0	3012	lobectomy	none	0
LNEN143TU	Typical	IA1	70	8,67	alive	0	4562	lobectomy	none	0
LNEN145TU	Typical	IB	53	6,11	alive	0	2137	lobectomy	none	0
LNEN146TU	Typical	IA2	73	6,69				lobectomy	none	0
LNEN148TU	Typical	IA1	69	6,54	alive	0	1112	lobectomy	none	0

0=alive; 1=dead

*0=no systemic treatment; 1=systemic treatment

Table S2: Validation cohort part 2

Patient	Histopathology	Stage	Age	*TERT*	OS (bin) #	OS (months)	Pre-op Chemotherapy*	Post-op chemotherapy*	Chemo or RT for recurrent disease*	Surgery *	Systemic Treatment *
Lu-Aty1	atypical	IA2	56	6,41	0	212,73	0	0	0	1	0
Lu-Aty10	atypical	IA3	52	10,3	1	171,23	0	0	0	1	0
Lu-Aty11	atypical	IA2	60	7,2	0	60,37	0	0	0	1	0
Lu-Aty12	atypical	IA3	74	12,06	1	99,17	0	0	0	1	0
Lu-Aty13	atypical	IIA	56	9,6	0	130,80	0	0	0	1	0
Lu-Aty2	atypical	IA2	61	6,6	1	41,53	0	0	Octreotide, bevacizumab	1	1
Lu-Aty3	typical	IIB	72	9,47	0	166,57	0	0	0	1	0
Lu-Aty4	atypical	IIIA	53	12,78	1	107,03	0	0	Platinum, etoposide, temozolomide	1	1
Lu-Aty5	atypical	IVA	61	13,63	1	72,53	1[a]	0	0	1	1
Lu-Aty6	atypical	IIIA	82	11,85	1	83,27	0	0	none (due to comorbidities)	1	0
Lu-Aty7	atypical	IIB	76	11,75	1	55,77	0	1 Adjuvant carboplatin, etoposide	RT, carboplatin, etoposide	1	1
Lu-Aty8	atypical	IIIA	81	10,96	1	125,60	0	1 Adjuvant concurrent platinum, etoposide, radiation	Brain metastasis resection and brain RT	1	1
Lu-Aty9	atypical	IIB	65	11,39	1	61,63	0	0	Octreotide, bevacizumab	1	1
Lu-ty1	typical	IA2	67	12,35	0	37,07	0	0	0	1	0
Lu-ty10	typical	IA1	66	6,22	0	132,13	0	0	0	1	0
Lu-ty11	typical	IB	63	5,56	0	15,53	0	0	0	1	0
Lu-ty12	typical	IB	28	5,82	0	64,87	0	0	0	1	0
Lu-ty13	typical	IA2	36	7,23	0	13,63	0	0	0	1	0
Lu-ty14	typical	IB	82	12,24	0	14,47	0	0	0	1	0
Lu-ty15	typical	IA2	74	6,12	1	45,17	0	0	0	1	0
Lu-ty16	typical	IA3	29	5,99	0	15,20	0	0	0	1	0
Lu-ty17	typical	IB	69	6,63	0	42,73	0	0	0	1	0
Lu-ty2	typical	IIIA	44	5,23	0	32,90	0	0	0	1	0
Lu-ty3	typical	IA2	67	9,73	1	126,23	0	0	0	1	0
Lu-ty4	typical	IA2	28	5,82	0	73,27	0	0	0	1	0
Lu-ty5	typical	IB	67	6,78	0	16,23	0	0	0	1	0

Lu-ty6	typical	IA3	34	5,29	0	33,00	0	0	0	1	0
Lu-ty7	typical	IIIA	35	6,51	0	132,40	0	0	0	1	0
Lu-ty8	typical	IA2	54	8,29	0	166,83	0	0	0	1	0
Lu-ty9	typical	IA3	68	5,7	0	130,93	0	0	0	1	0

[a] Patient presented with stage IV disease. Was treated with systemic chemotherapy (paclitaxel+ carboplatin; then etoposide+carboplatin; then octreotide; ten AKT1 inhibitor). Lung tumor resection was performed for palliative purposes

0=alive; 1=dead

*0=no; 1=yes

Table S3: Crosstable for the occurrence of risk factors *TERT* expression (*TERT* high/low) and histology (atypical/typical carcinoids) within the test cohort.

	Typical carcinoids	Atypical carcinoids	Total number
TERT low	50 (82%)	11 (18%)	61
TERT high	8 (34,8%)	15 (65,2%)	23

Table S4: Crosstable for the occurrence of risk factors *TERT* expression (*TERT* high/low) and stage (≤ stage IIA/≥ stage IIB) within the test cohort.

	Stage ≤ IIA	Stage ≥ IIB	Total number
TERT low	52 (88.1%)	7 (11.9%)	59
TERT high	14 (56%)	11 (44%)	25

Table S5: Crosstable for the occurrence of risk factors *TERT* expression (*TERT* high/low) and histology (atypical/typical carcinoids) within the validation cohort.

	Typical carcinoids	Atypical carcinoids	Total number
TERT low	44 (81.5%)	10 (18.5%)	54
TERT high	21 (42.0%)	29 (58.0%)	50

Table S6: Crosstable for the occurrence of risk factors *TERT* expression (*TERT* high/low) and stage (≤ stage IIA/≥ stage IIB) within the validation cohort.

	Stage ≤ IIA	Stage ≥ IIB	Total number
TERT low	36 (72.0%)	14 (28.0%)	50
TERT high	30 (63.8%)	17 (36.2%)	47

Table S7: Univariate analysis

Variable	**Patients analyzed**	**HR univariate**	***P*-value**
Stage (≥IIB and ***≤IIA***)	≤IIA n= 115 ≥IIB n= 45	2.599 (95% CI 1.264-5.343)	0.009
Stage (≥III and ***≤II***)	≤II n= 136 ≥III n=24	2.675 (95% CI 1.239-5.771)	0.012
Stage (≥IIIB and ***≤IIIA***)	≤IIIA n= 152 ≥IIIB n= 8	5.071 (95% CI 2.044-12.582)	<0.001
Histology (atypical and ***typical***)	TC n=102 AC n=58	4.207 (95% CI 1.711-10.346)	0.002

Table S8: Multivariable analysis for overall survival, considering the risk factors *TERT* expression, stage (≤II versus ≥III), and histology (backward selection)

Variable	Patients analyzed	HR univariate	*P*-value	HR multivariable*	*P*-value
TERT expression (high >8.17 and low ***≤8.17***)	Low n=96 High n=64	6.884 (95% CI 2.622-18.071)	<0.001	5.243 (95% CI 1.943-14.148)	0.001
Stage (≥III and ***≤II***)	≤II n=136 ≥III n= 24	2.675 (95% CI 1.239-5.771)	0.012		
Histology (atypical and ***typical***)	TC n=102 AC n=58	4.207 (95% CI 1.711-10.346)	0.002	2.639 (95% CI 1.048-6.644)	0.039

HR, hazard ratio. *hazard ratios derived by multivariable backward selection; interaction of *TERT* expression and histology was included in multivariable analysis but excluded during backward selection.

Table S9: Multivariable analysis for overall survival, considering the risk factors *TERT* expression, stage (≤IIIA versus ≥IIIB), and histology (backward selection).

Variable	Patients analyzed	HR univariate	*P*-value	HR multivariable*	*P*-value
TERT expression (high >8.17 and low ***≤8.17***)	Low n=96 High n=64	6.884 (95% CI 2.622-18.071)	<0.001	5.243 (95% CI 1.943-14.148)	0.001
Stage (≥IIIB and ***≤IIIA***)	≤IIIA n=152 ≥IIIB n= 8	5.071 (95% CI 2.044-12.582)	<0.001		
Histology (atypical and ***typical***)	TC n=102 AC n=58	4.207 (95% CI 1.711-10.346)	0.002	2.639 (95% CI 1.048-6.644)	0.039

HR, hazard ratio. *hazard ratios derived by multivariable backward selection; interaction of *TERT* expression and histology was included in multivariable analysis but excluded during backward selection.

Table S10: Multivariable analysis for overall survival, considering the risk factors *TERT* expression, stage (≤IIA versus ≥IIB), and histology (backward selection); threshold based on neuroblastoma dataset (NB-cutoff).

Variable	**Patients analyzed**	**HR univariate**	***P*-value**	**HR multivariable***	***P*-value**
TERT expression (high >7.58 and low ***≤7.58***)	Low n=88 High n=72	5.371 (95% CI 2.039-14.146)	<0.001	3.976 (95% CI 1.469-10.763)	0.007
Stage (≥IIB and ***≤IIA***)	≤IIA n=115 ≥IIB n= 45	2.599 (95% CI 1.264-5.343	0.009		
Histology (atypical and ***typical***)	TC n=102 AC n=58	4.207 (95% CI 1.711-10.346)	0.002	2.882 (95% CI 1.146-7.251)	0.025

HR, hazard ratio. *hazard ratios derived by multivariable backward selection; interaction of *TERT* expression and histology was included in multivariable analysis but excluded during backward selection.

Table S11: Multivariable analysis for overall survival, considering the risk factors *TERT* expression, stage (≤II versus ≥III), and histology (backward selection)

Variable	**Patients analyzed**	**HR univariate**	***P*-value**	**HR multivariable***	***P*-value**
TERT expression (high >7.58 and low ***≤7.58***)	Low n=88 High n=72	5.371 (95% CI 2.039-14.146)	<0.001	3.976 (95% CI 1.469-10.763)	0.007
Stage (≥III and ***≤II***)	≤II n=136 ≥III n=24	2.675 (95% CI 1.239-5.771)	0.012		
Histology (atypical and ***typical***)	TC n=102 AC n=58	4.207 (95% CI 1.711-10.346)	0.002	2.882 (95% CI 1.146-7.251)	0.025

HR, hazard ratio. *hazard ratios derived by multivariable backward selection; interaction of *TERT* expression and histology was included in multivariable analysis but excluded during backward selection.

Table S12: Multivariable analysis for overall survival, considering the risk factors *TERT* expression, stage (≤IIIA versus ≥IIIB), and histology (backward selection).

Variable	**Patients analyzed**	**HR univariate**	***P*-value**	**HR multivariable***	***P*-value**
TERT expression (high >7.58 and low ***≤7.58***)	Low n=88 High n=72	5.371 (95% CI 2.039-14.146)	<0.001	3.564 (95% CI 1.287-9.873)	0.014
Stage (≥IIIB and ***≤IIIA***)	≤IIIA n=152 ≥IIIB n=8	5.071 (95% CI 2.044-12.582)	<0.001	2.383 (95% CI 0.928-6.121)	0.071

Histology (atypical and ***typical***)	TC n=102 AC n=58	4.207 (95% CI 1.711-10.346)	0.002	2.566 (95% CI 0.998-6.599)	0.050

HR, hazard ratio *hazard ratios derived by multivariable backward selection; interaction of *TERT* expression and histology was included in multivariable analysis but excluded during backward selection.

Table S13: Information on *TERT* copy number status (validation cohort).

Sample_ID	**Copy number**	**Copy number rounded**	**Minor allele Copy number**	**Minor allele Copy number rounded**	**Category**
LNEN047	4.7285	5	1.7755	2	Amplified
LNEN048	1.9984	2	0.9917	1	Normal
LNEN050	1.9978	2	0.9933	1	Normal
LNEN051	2.9888	3	0.9908	1	Amplified
LNEN055	3.039	3	1.0148	1	Amplified
LNEN056	4.9784	5	1.9777	2	Amplified
LNEN057	4.0259	4	1.9966	2	Amplified
LNEN060	2.0209	2	0.9978	1	Normal
LNEN063	2.0031	2	0.9865	1	Normal
LNEN064	2.0042	2	0.9786	1	Normal
LNEN066	2.0093	2	0.9986	1	Normal
LNEN067	2.009	2	0.9891	1	Normal
LNEN068	1.9812	2	0.9661	1	Normal
LNEN071	2.9882	3	0.9941	1	Amplified
LNEN072	2.9806	3	0.9965	1	Amplified
LNEN074	2.0001	2	0.9965	1	Normal
LNEN076	1.9882	2	0.9851	1	Normal
LNEN077	1.996	2	0.9846	1	Normal
LNEN081	1.9855	2	0.9709	1	Normal
LNEN083	2.0556	2	0.9991	1	Normal
LNEN084	2.0212	2	0.9979	1	Normal
LNEN089	2.0018	2	0.9983	1	Normal

LNEN092	2.0034	2	0.9814	1	Normal
LNEN093	2.0092	2	0.9885	1	Normal
LNEN094	2.9891	3	0.9953	1	Amplified
LNEN095	4.6255	5	2.0837	2	Amplified
LNEN096	3.0082	3	1.0067	1	Amplified
LNEN097	2.2349	2	0.9901	1	Normal
LNEN100	2.0145	2	0.9876	1	Normal
LNEN104	2.0003	2	0.9976	1	Normal
LNEN106	2.0264	2	0.9976	1	Normal
LNEN107	1.9856	2	0.9746	1	Normal
LNEN108	2.0066	2	0.9918	1	Normal
LNEN109	2.0117	2	0.9939	1	Normal
LNEN110	2.0135	2	0.9956	1	Normal
LNEN111	2.0047	2	0.9989	1	Normal
LNEN112	2.0707	2	0.9794	1	Normal
LNEN113	2.0336	2	0.9719	1	Normal
LNEN114	2.242	2	0.9964	1	Normal
LNEN115	3.0744	3	1.0141	1	Amplified
LNEN116	1.9884	2	0.9858	1	Normal
LNEN117	2.0081	2	0.9885	1	Normal
LNEN118	2.9879	3	0.9907	1	Amplified
LNEN119	4.1051	4	1.988	2	Amplified
LNEN121	2.0065	2	0.9985	1	Normal
LNEN123	2.0293	2	0.9988	1	Normal
LNEN125	2.0036	2	0.9987	1	Normal
LNEN126	3.001	3	0.9986	1	Amplified
LNEN130	1.9874	2	0.9857	1	Normal
LNEN132	3.0085	3	1.0003	1	Amplified
LNEN133	1.9859	2	0.9847	1	Normal
LNEN135	2.0012	2	0.998	1	Normal
LNEN136	1.9993	2	0.9946	1	Normal
LNEN139	1.9893	2	0.9862	1	Normal
LNEN140	1.9933	2	0.9925	1	Normal

LNEN142	2.0001	2	0.998	1	Normal
LNEN143	2.0086	2	0.999	1	Normal
LNEN145	2.0396	2	0.9967	1	Normal
LNEN146	1.9948	2	0.992	1	Normal

Table S14: Crosstable for the occurrence of *TERT* expression (*TERT* high/low) and *TERT* copy number (normal/amplified) within the validation cohort.

***TERT* expression**		***TERT* copy number normal**	***TERT* copy number amplified**
TERT high	Numbers	21	7
TERT low	Numbers	23	8
Fisher's exact test		>0.9	

Table S15:

Patient	**Cohort***	***TERT*_cg11625005_methylation_beta_value**
LNEN002	test cohort	0,615
LNEN003	test cohort	0,617
LNEN004	test cohort	0,572
LNEN005	test cohort	0,75
LNEN006	test cohort	0,835
LNEN007	test cohort	0,922
LNEN008	test cohort	NA
LNEN009	test cohort	0,909
LNEN010	test cohort	0,933
LNEN011	test cohort	0,81
LNEN012	test cohort	NA
LNEN013	test cohort	0,84
LNEN014	test cohort	0,639
LNEN015	test cohort	0,804
LNEN016	test cohort	0,656
LNEN017	test cohort	0,931
LNEN018	test cohort	NA
LNEN019	test cohort	NA
LNEN020	test cohort	0,883
S00076	test cohort	0,749
S01513	test cohort	NA
S01572	test cohort	0,921
S02331	test cohort	NA
S02335	test cohort	NA
S00716	test cohort	NA
S02126	test cohort	NA
S01519	test cohort	NA
S01103_T2	test cohort	0,9
S01504	test cohort	NA
S02340	test cohort	NA
S01520	test cohort	NA
S01202	test cohort	0,853
S00016	test cohort	0,908
S02323	test cohort	NA
S02337	test cohort	NA
S01593	test cohort	NA

S00516	test cohort	0,713
S02162	test cohort	NA
S01528	test cohort	0,909
S00520	test cohort	0,744
S01605	test cohort	0,673
S00858	test cohort	NA
S02327	test cohort	0,882
S01573	test cohort	0,763
S01536	test cohort	NA
S01546	test cohort	0,731
S01746	test cohort	NA
S01731	test cohort	NA
S02330	test cohort	0,721
S01493	test cohort	NA
S02334	test cohort	NA
S01501	test cohort	NA
S01666	test cohort	0,722
S01539	test cohort	0,684
S01742	test cohort	NA
S01531	test cohort	NA
S02154	test cohort	NA
S01060	test cohort	0,733
S01538	test cohort	0,775
S01515	test cohort	NA
S01567	test cohort	NA
S01502	test cohort	0,799
S00128	test cohort	0,589
S01583	test cohort	0,673
S01733	test cohort	NA
S02325	test cohort	NA
S01537	test cohort	NA
S00515	test cohort	0,737
S01540	test cohort	0,797
S01529	test cohort	0,69
S02333	test cohort	NA
S01585	test cohort	NA
S00118	test cohort	0,87
S01526	test cohort	NA
S00094	test cohort	0,76
S01532	test cohort	0,567
S01582	test cohort	0,695
S01543	test cohort	0,747
S01545	test cohort	0,866
S00089	test cohort	0,561
S01510	test cohort	NA
S01541	test cohort	0,717
S02326	test cohort	NA
S01590	test cohort	0,501
S01521	test cohort	0,75

S02339	test cohort	NA
S01584	test cohort	NA
S02338	test cohort	NA
Lu_Aty1	validation cohort part 2	NA
Lu_Aty10	validation cohort part 2	NA
Lu_Aty11	validation cohort part 2	0,349
Lu_Aty12	validation cohort part 2	0,925
Lu_Aty13	validation cohort part 2	NA
Lu_Aty2	validation cohort part 2	NA
Lu_Aty3	validation cohort part 2	0,596
Lu_Aty4	validation cohort part 2	0,738
Lu_Aty5	validation cohort part 2	NA
Lu_Aty6	validation cohort part 2	NA
Lu_Aty7	validation cohort part 2	0,77
Lu_Aty8	validation cohort part 2	0,806
Lu_Aty9	validation cohort part 2	0,902
Lu_ty1	validation cohort part 2	NA
Lu_ty10	validation cohort part 2	0,83
Lu_ty11	validation cohort part 2	0,757
Lu_ty12	validation cohort part 2	NA
Lu_ty13	validation cohort part 2	0,787
Lu_ty14	validation cohort part 2	0,883
Lu_ty15	validation cohort part 2	0,816
Lu_ty16	validation cohort part 2	0,69
Lu_ty17	validation cohort part 2	0,167
Lu_ty2	validation cohort part 2	0,78

Lu_ty3	validation cohort part 2	0,845
Lu_ty4	validation cohort part 2	0,766
Lu_ty5	validation cohort part 2	0,688
Lu_ty6	validation cohort part 2	NA
Lu_ty7	validation cohort part 2	NA
Lu_ty8	validation cohort part 2	NA
Lu_ty9	validation cohort part 2	NA

*no DNA methylation data available for validation cohort part 1

References:

1. Fernandez-Cuesta L, Peifer M, Lu X, et al: Frequent mutations in chromatin-remodelling genes in pulmonary carcinoids. Nat Commun 5:3518, 2014
2. Alcala N, Leblay N, Gabriel AAG, et al: Integrative and comparative genomic analyses identify clinically relevant pulmonary carcinoid groups and unveil the supra-carcinoids. Nat Commun 10:3407, 2019
3. Laddha SV, da Silva EM, Robzyk K, et al: Integrative Genomic Characterization Identifies Molecular Subtypes of Lung Carcinoids. Cancer Res 79:4339-4347, 2019
4. Peifer M, Hertwig F, Roels F, et al: Telomerase activation by genomic rearrangements in high-risk neuroblastoma. Nature 526:700-4, 2015
5. Peng X, Thierry-Mieg J, Thierry-Mieg D, et al: Tissue-specific transcriptome sequencing analysis expands the non-human primate reference transcriptome resource (NHPRTR). Nucleic Acids Res 43:D737-42, 2015
6. Newman AM, Steen CB, Liu CL, et al: Determining cell type abundance and expression from bulk tissues with digital cytometry. Nat Biotechnol 37:773-782, 2019
7. Ackermann S, Cartolano M, Hero B, et al: A mechanistic classification of clinical phenotypes in neuroblastoma. Science 362:1165-1170, 2018
8. Cun Y, Yang TP, Achter V, et al: Copy-number analysis and inference of subclonal populations in cancer genomes using Sclust. Nat Protoc 13:1488-1501, 2018
9. Huang Y, Yang X, Lu T, et al: Assessment of the prognostic factors in patients with pulmonary carcinoid tumor: a population-based study. Cancer Med 7:2434-2441, 2018
10. Cardillo G, Sera F, Di Martino M, et al: Bronchial carcinoid tumors: nodal status and long-term survival after resection. Ann Thorac Surg 77:1781-5, 2004
11. Baudin E, Caplin M, Garcia-Carbonero R, et al: Lung and thymic carcinoids: ESMO Clinical Practice Guidelines for diagnosis, treatment and follow-up(). Ann Oncol 32:439-451, 2021
12. Cesare AJ, Heaphy CM, O'Sullivan RJ: Visualization of Telomere Integrity and Function In Vitro and In Vivo Using Immunofluorescence Techniques. Curr Protoc Cytom 73:12 40 1-12 40 31, 2015
13. Caplin ME, Baudin E, Ferolla P, et al: Pulmonary neuroendocrine (carcinoid) tumors: European Neuroendocrine Tumor Society expert consensus and recommendations for best practice for typical and atypical pulmonary carcinoids. Ann Oncol 26:1604-20, 2015
14. Yoon JY, Sigel K, Martin J, et al: Evaluation of the Prognostic Significance of TNM Staging Guidelines in Lung Carcinoid Tumors. J Thorac Oncol 14:184-192, 2019
15. Centonze G, Maisonneuve P, Simbolo M, et al: Lung carcinoid tumours: histology and Ki-67, the eternal rivalry. Histopathology 82:324-339, 2023
16. Meeser A, Bartenhagen C, Werr L, et al: Reliable assessment of telomere maintenance mechanisms in neuroblastoma. Cell Biosci 12:160, 2022